PB82-250127

Evaluation of a Simulated Road Texture for the Testing of Tire/Road Noise

Wyle Labs./Wyle Research
Arlington, VA

Prepared for

Environmental Protection Agency
Arlington, VA

Mar 82

U.S. Department of Commerce
National Technical Information Service
NTIS

PB82-250127

United States Environmental
Protection Agency

Office of Noise Abatement
and Control
Washington, D.C. 20460

EPA REPORT NO. 550/9-82-332

EVALUATION OF A SIMULATED ROAD TEXTURE FOR THE TESTING OF TIRE/ROAD NOISE

MARCH 1982

REPRODUCED BY
NATIONAL TECHNICAL
INFORMATION SERVICE
U.S. DEPARTMENT OF COMMERCE
SPRINGFIELD, VA. 22161

TECHNICAL REPORT DATA
Please read Instructions on the reverse before completing

1. REPORT NO.	2.	3. RECIPIENT'S ACCESSION NO.
550/9-82-332		PB82 250127

4. TITLE AND SUBTITLE	5. REPORT DATE
Evaluation of a Simulated Road Texture for the Testing of Tire/Road Noise	March 1982
	6. PERFORMING ORGANIZATION CODE

7. AUTHOR(S)	8. PERFORMING ORGANIZATION REPORT NO.
Eric Stusnick, Kenneth J. Plotkin	WR 82-3

9. PERFORMING ORGANIZATION NAME AND ADDRESS	10. PROGRAM ELEMENT NO.
Wyle Labortories / Wyle Research 2361 Jefferson Davis Highway, Suite PL-404 Arlington, Virginia 22202	11. CONTRACT/GRANT NO. 68-01-6243

12. SPONSORING AGENCY NAME AND ADDRESS	13. TYPE OF REPORT AND PERIOD COVERED
U.S. Environmental Protection Agency Office of Noise Abatement and Control 1921 Jefferson Davis Highway Arlington, Virginia 22202	Interim Task
	14. SPONSORING AGENCY CODE

15. SUPPLEMENTARY NOTES

16. ABSTRACT

As part of a project to study tire/road noise, a laboratory roadwheel facility was equipped with replica road surfaces. The replica surfaces, of a design first developed by Dunlop, Ltd., consisted of fiberglass and epoxy resin shells clamped to the roadwheel. The outer surface of each shell was molded from a rubber impression taken from a real road surface, thus replicating the texture. To evaluate the effect of pavement texture, and to establish the realism of the replica surfaces, a series of near-field measurements of noise from four heavy truck tires were made on the replica surfaces and on moving tests on the real surfaces. Moving tests on a flat steel surface were also made. Data from these same tires on a smooth steel roadwheel were available from a previous program. A comparison between these three sets of data shows that the replica surface provides a good simulation of real pavement, and is more realistic than a plain steel drum. The conclusion was also reached that in laboratory facilities it is more important to duplicate the road texture than the curvature of the surface.

17. KEY WORDS AND DOCUMENT ANALYSIS

a. DESCRIPTORS	b. IDENTIFIERS/OPEN ENDED TERMS	c. COSATI Field/Group
Tire Noise Noise Models Transportation Noise		

18. DISTRIBUTION STATEMENT	19. SECURITY CLASS (This Report)	21. NO. OF PAGES
Unlimited	UNCLASSIFIED	
	20. SECURITY CLASS (This page)	22. PRICE
	UNCLASSIFIED	

EPA Form 2220-1 (9-73)

ACKNOWLEDGMENTS

The authors would like to thank Messrs. Doug Van Arnam and Mike Roth, of Smithers Scientific Services, for their outstanding assistance during the outdoor and roadwheel tests.

We gratefully thank Dunlop, Ltd., for their generosity and openness in sharing their technology and experience with the resin replica road shells. We would like to thank Drs. C.W. Barson and J.C. Walker of Dunlop for their hospitality in demonstrating the replicas at their laboratory. We also thank Mr. Peter D. Hartley for his excellent work in manufacturing the replica surfaces.

A number of people from the tire industry generously provided review and comments on a preliminary presentation of the work described in this report. We would like to thank: Marion Pottinger and Donald Thrasher of BFGoodrich; Leonard Charek, Ray Griggy, Sunil Jha, and Paul Sekula of Firestone; Frank Matyja of General Tire; and Bill Hnat of Goodyear.

This report has been approved for general availability. The contents of this report reflect the views of the contractor, who is responsible for the facts and the accuracy of the data presented herein, and do not necessarily reflect the official views or policy of the EPA or the tire industry. This report does not constitute a standard, specification, or regulation.

TABLE OF CONTENTS

		Page
1.0	INTRODUCTION	1
2.0	ROADWHEEL WITH SIMULATED PAVEMENT	3
3.0	EXPERIMENTAL PROCEDURES	12
3.1	Test Tires	12
3.2	Field Measurements	12
3.3	Roadwheel Measurements	31
3.4	Data Reduction and Analysis	34
4.0	EXPERIMENTAL RESULTS	36
4.1	Analysis of A-Weighted Sound Levels	36
4.1.1	Effects of Carcass and Tread Design	36
4.1.2	Effects of Roadway Surface	40
4.1.3	Comparison of Roadway and Roadwheel Results	46
4.1.4	Comparison of Steel Plate and Steel Roadwheel Results	56
4.2	Spectra and Time Signatures	64
4.2.1	Spectra	64
4.2.2	Time Signatures	66
5.0	CONCLUSIONS	74
REFERENCES		R-1

LIST OF TABLES

Table No.		Page
1	Surface Curvature/Texture Matrix	2
2	Selection of Test Tire Designs	13
3	Test Tire Specifications	13
4	Coastby Test Matrix for Each Tire	30
5	Summary of Noisiest and Quietest Tire Types	39
6	Summary of Noisiest and Quietest Roadway Surfaces	45

LIST OF FIGURES

Fig. No.		Page
1	Endurance Wheel Noise Test Facility	4
2	Making Rubber Impression of Pavement	6
3	Replica Asphalt Texture	7
4	Replica Concrete Texture	7
5	Floating Replica Shell to Roadwheel	8
6	Attachment of Replica Shells Via Clamps	9
7	Interior of Acoustic Chamber	11
8	Test Tires (Bias Rib, Bias Crossbar, Radial Rib, Radial Lug)	14
9	Footprint of Tire #1 -- Radial Lug	15
10	Footprint of Tire #2 -- Radial Rib	15
11	Footprint of Tire #3 -- Bias Crossbar	16
12	Footprint of Tire #4 -- Bias Rib	16
13	Instrumentation for Outdoor Tests	17
14	Test Tire on Vehicle, With Microphones in Position	19
15	Accelerometer Mount Design	21
16	Test Vehicle on VDA	22
17	Test Vehicle Approaching Flat Steel Plate	23
18	Skid Pad at Ohio TRC	25
19	Vehicle Dynamics Area at TRC	25
20	Unsealed Asphalt (A1)	26
21	Sealed Asphalt (A2)	26
22	Medium ("Interstate") Concrete (C1)	28
23	Smooth Concrete (C2)	28
24	Rough Concrete (C3)	29
25	Steel Plate (S)	29

LIST OF FIGURES (Continued)

Fig. No.		Page
26	Instrumentation for Roadwheel Measurements	32
27	Instrumentation System in Place at Roadwheel	33
28	Instrumentation for Data Reduction	35
29	A-Weighted Sound Level Versus Vehicle Speed as a Function of Tire Type for Concrete Surface (C1)	37
30	A-Weighted Sound Level Versus Vehicle Speed as a Function of Tire Type for Asphalt Surface (A1)	38
31	A-Weighted Sound Level Versus Vehicle Speed as a Function of Roadway Surface for Radial Rib Tire	41
32	A-Weighted Sound Level Versus Vehicle Speed as a Function of Roadway Surface for Radial Lug Tire	42
33	A-Weighted Sound Level Versus Vehicle Speed as a Function of Roadway Surface for Bias Rib Tire	43
34	A-Weighted Sound Level Versus Vehicle Speed as a Function of Roadway Surface for Bias Crossbar Tire	44
35(a)	A-Weighted Sound Level Versus Vehicle Speed as a Function of Surface Type for Radial Rib Tire and Concrete Surfaces	47
35(b)	A-Weighted Sound Level Versus Vehicle Speed as a Function of Surface Type for Radial Rib Tire and Asphalt Surfaces	48
36(a)	A-Weighted Sound Level Versus Vehicle Speed as a Function of Surface Type for Radial Lug Tire and Concrete Surfaces	49
36(b)	A-Weighted Sound Level Versus Vehicle Speed as a Function of Surface Type for Radial Lug Tire and Asphalt Surfaces	50
37(a)	A-Weighted Sound Level Versus Vehicle Speed as a Function of Surface Type for Bias Rib Tire and Concrete Surfaces	51
37(b)	A-We.ghted Sound Level Versus Vehicle Speed as a Function of Surface Type for Bias Rib Tire and Asphalt Surfaces	52
38(a)	A-Weighted Sound Level Versus Vehicle Speed as a Function of Surface Type for Bias Crossbar Tire and Concrete Surfaces	53
38(b)	A-Weighted Sound Level Versus Vehicle Speed as a Function of Surface Type for Bias Crossbar Tire and Asphalt Surfaces	54

LIST OF FIGURES (Continued)

Fig. No.		Page
39	Best Linear Fit of Roadway Levels to Roadwheel Levels for All Tires, Boat Roadway Surfaces, All Vehicle Speeds, and All Microphone Positions . .	55
40	Best Unit-Slope Linear Fit of Roadway Levels to Roadwheel Levels for All Tires, Both Roadway Surfaces, All Vehicle Speeds, and All Microphone Positions	56
41	Best Unit-Slope Linear Fit of Roadway Levels to Roadwheel Levels for All Tires, Both Roadway Surfaces, All Vehicle Speeds, and Microphone 3 Only	57
42	A-Weighted Sound Level Versus Vehicle Speed as a Function of Surface Curvature for Radial Rib Tire	59
43	A-Weighted Sound Level Versus Vehicle Speed as a Function of Surface Curvature for Radial Lug Tire	60
44	A-Weighted Sound Level Versus Vehicle Speed as a Function of Surface Curvature for Bias Rib Tire	61
45	A-Weighted Sound Level Versus Vehicle Speed as a Function of Surface Curvature for Bias Crossbar Tire	62
46	Best Linear Fit of Flat Steel Plate Levels to Steel Roadwheel Levels for All Tires, All Microphone Positions, and Two Vehicle Speeds	63
47	Best Unit-Slope Linear Fit of Flat Steel Plate Levels to Steel Roadwheel Levels for All Tires, All Microphone Positions, and Two Vehicle Speeds . . .	63
48	Comparison of Spectra on Real, Replica, and Steel Surfaces	65
49	Successive Samples of Sound Pressure on Steel Roadwheel	67
50	Successive Samples of Carcass Acceleration on Steel Roadwheel	68
51	Successive Samples of Sound Pressure on Replica Surface	69
52	Successive Samples of Carcass Acceleration on Replica Surface	70
53	Successive Samples of Sound Pressure on Real Surface	71
54	Successive Samples of Carcass Acceleration on Real Surface	72

1.0 INTRODUCTION

As part of a program to develop techniques for quieting heavy truck tires, a unified set of theoretical noise models has been prepared.[1] The physical foundation of these models is based to a large degree on an earlier experimental study,[2] in which near-field sound and carcass vibration of several production truck tires were measured on a smooth steel roadwheel. The next stage of development of the noise models is to refine and validate them experimentally, utilizing a set of specially constructed tires. Since it is well known that pavement texture has a significant effect on tire noise,[3,4,5,6,7,8,9,10] the noise models include theoretical effects of texture. In order to properly test these elements of the models, the experimental program must include texture. It was decided to add simulated texture to the roadwheel facility, using the plastic replica shell method successfully used by Dunlop.[9,10] This method consists of attaching to the roadwheel cast resin shells whose outer surface is molded from rubber impressions of a real road surface.

In order to evaluate fully the validity of the test facility, several sets of measurements were performed and compared:

- Outdoor noise measurements were made on a variety of surfaces, utilizing the four production tires previously tested on the steel roadwheel.[2] Transducer positions and test conditions duplicated as closely as possible those of the roadwheel tests. Data were collected for five road surfaces (two of which were used as models for resin replica shells) and a flat steel plate. The steel plate was incorporated to provide an evaluation of the effects of curvature, which has been of some concern in roadwheel testing.[11,12]
- Indoor measurements on the roadwheel facility with two replica surfaces, using the same tires and transducer arrangement.
- Data from these same tires from the previous program,[2] collected on the smooth steel roadwheel.

This report serves two purposes. The first is to document the effects of curvature and texture on noise insomuch as it affects the validity of the modified roadwheel facility. Table I illustrates the surface curvature/texture matrix on which this evaluation is made. The second purpose is to document the outdoor noise measurements. While not central to the question of facility validity, these data form an empirical study of five pavements and four tires which adds to the body of work included in References 3 through 10.

Section 2 of this report describes the roadwheel test facility and the pavement simulation. Section 3 describes the measurements conducted, both indoors and outdoors. Section 4 is an analysis of the data. Conclusions of this study are summarized in Section 5.

Table I

Surface Curvature/Texture Matrix

		SURFACE CURVATURE	
		Curved	Flat
SURFACE TEXTURE	Steel	SMOOTH STEEL ROADWHEEL	STEEL PLATE FASTENED TO CONCRETE ROADWAY
	Concrete	REPLICA RESIN MOLD OF CONCRETE SURFACE ATTACHED TO ROADWHEEL	INTERSTATE CONCRETE ROADWAY
	Asphalt	REPLICA RESIN MOLD OF ASPHALT SURFACE ATTACHED TO ROADWHEEL	UNSEALED ASPHALT ROADWAY

2.0 ROADWHEEL WITH SIMULATED PAVEMENT

The roadwheel measurements were carried out on the truck tire machine at the CTI Division of Smithers Scientific Services in Ravenna, Ohio. The machine is a 67-inch-diameter smooth steel roadwheel endurance testing facility, capable of loads up to 10,000 pounds and speeds from 5 to 120 mph. This facility was used by Wyle in the previous program of tire noise evaluation.[2] The complete machine consists of two wheels (driven by toothed belts from electric motors) and four test stations. For the previous tire noise measurements, a semi-anechoic chamber had been constructed about one test station. This chamber, which had been disassembled and stored at the conclusion of that program, was reinstalled on the roadwheel machine and acoustic qualification tests were performed to validate its performance. An illustration of the modified roadwheel facility is shown in Figure 1.

The walls and ceiling of the chamber are constructed of 1/2- and 1/4-inch plywood spot-bonded together. This construction was designed to shield noise from the drive belt, tires on other stations, and other machinery within the laboratory. In general, one-third octave band background noise levels in the audio frequency range within the chamber are below 65 dB with the machine operating at 60 mph. The walls of the chamber are lined with 6 inches of Owens-Corning 703 Fiberglas. The wall adjacent to the roadwheel is not lined with Fiberglas, and has a hole large enough to accommodate the contact patch of the tire against the roadwheel. This wall formed a simulated hard, reflective ground plane. The interior dimensions of this semi-anechoic chamber are approximately 6 feet by 7 feet by 5 feet.

For the current program, the facility was further modified by the addition of simulated pavement texture. The method used was that successfully employed by Dunlop, Ltd., in Birmingham, England.[9] This method consists of attaching to the roadwheel sets of cast resin shells whose outer surfaces were molded from rubber impressions of actual road surfaces. The surfaces were made for Dunlop by Mr. Peter Hartley, a pattern and model maker specializing in plastics. A visit was made to Dunlop's research laboratory to examine their surfaces, and Mr. Hartley was engaged to make surfaces to fit the roadwheel at Smithers.

The manufacturing process of the surfaces consisted of the following steps:

1. Cold-cured flexible rubber impressions were made of two road surfaces. Each impression was made over an area slightly larger than the width and circumference of the roadwheel. Impressions were made of one concrete and one

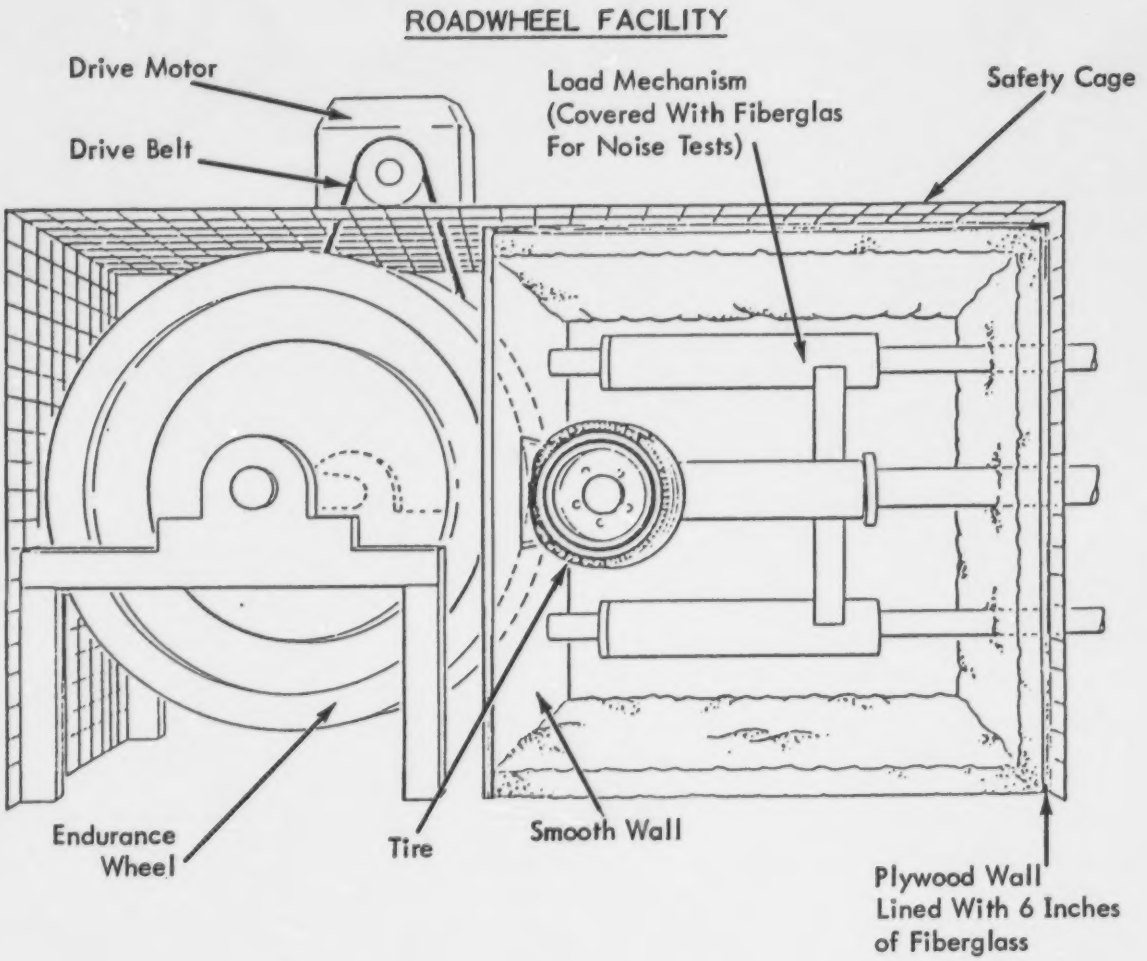

Figure 1. Endurance Wheel Noise Test Facility.

asphalt surface over which coasting tests were conducted. (See Section 3 for a detailed description of the surfaces.) Figure 2 shows the rubber impression process.

2. An inner mold was constructed which duplicates the outer surface of the roadwheel.

3. A temporary spacer, equal to the desired shell thickness, was wrapped around the inner mold. The rubber impression was wrapped around this, pavement-texture side in, and was trimmed to the width of the roadwheel.

4. Hard casting resin was poured around the rubber impression, forming an outer mold with the rubber imbedded.

5. The temporary spacer between the inner and outer mold was removed and a fiberglass-reinforced resin shell was cast, and divided into three 120-degree segments. The outer surface of this shell is a silicon resin which simulates the hardness of pavement. Figures 3 and 4 are photographs of the final surfaces.

6. The shells were clamped onto the roadwheel. To ensure a perfect fit, the initial installation employed a floating process, wherein a thin layer of resin was placed between the shell and the wheel. The joints between segments were carefully aligned, and the resin allowed to cure. Subsequent installation of the shells was always done aligned to a fixed circumferential reference. Figures 5 and 6 show the floating process. The roadwheel and clamps were waxed prior to floating so that the resin would not stick to them.

The use of clamps to attach the shells was a departure from the design at Dunlop, where the shells were attached with capscrews into existing holes in the roadwheel. No holes were present in the roadwheel at Smithers. Six holes (two for each segment) were drilled to provide positive alignment of the shells, and 84 specially designed clamps were used. The clamps are visible in Figure 6. Keyed recesses (visible in Figures 3 through 5) were molded into the shells to positively align the clamps. During installation, the clamps were tightened with a calibrated torque wrench to ensure a uniform prestress to about three times the centripital load at 50 mph.

The roadwheel opening in the simulated ground plane was widened so as to accommodate the added width of the clamps. A layer of 3/4-inch plywood was also added to match the thickness of the shells.

A serious acoustical problem encountered was a turbine-like noise generated at harmonics of the clamp passage frequency, due to interaction between the clamps and the

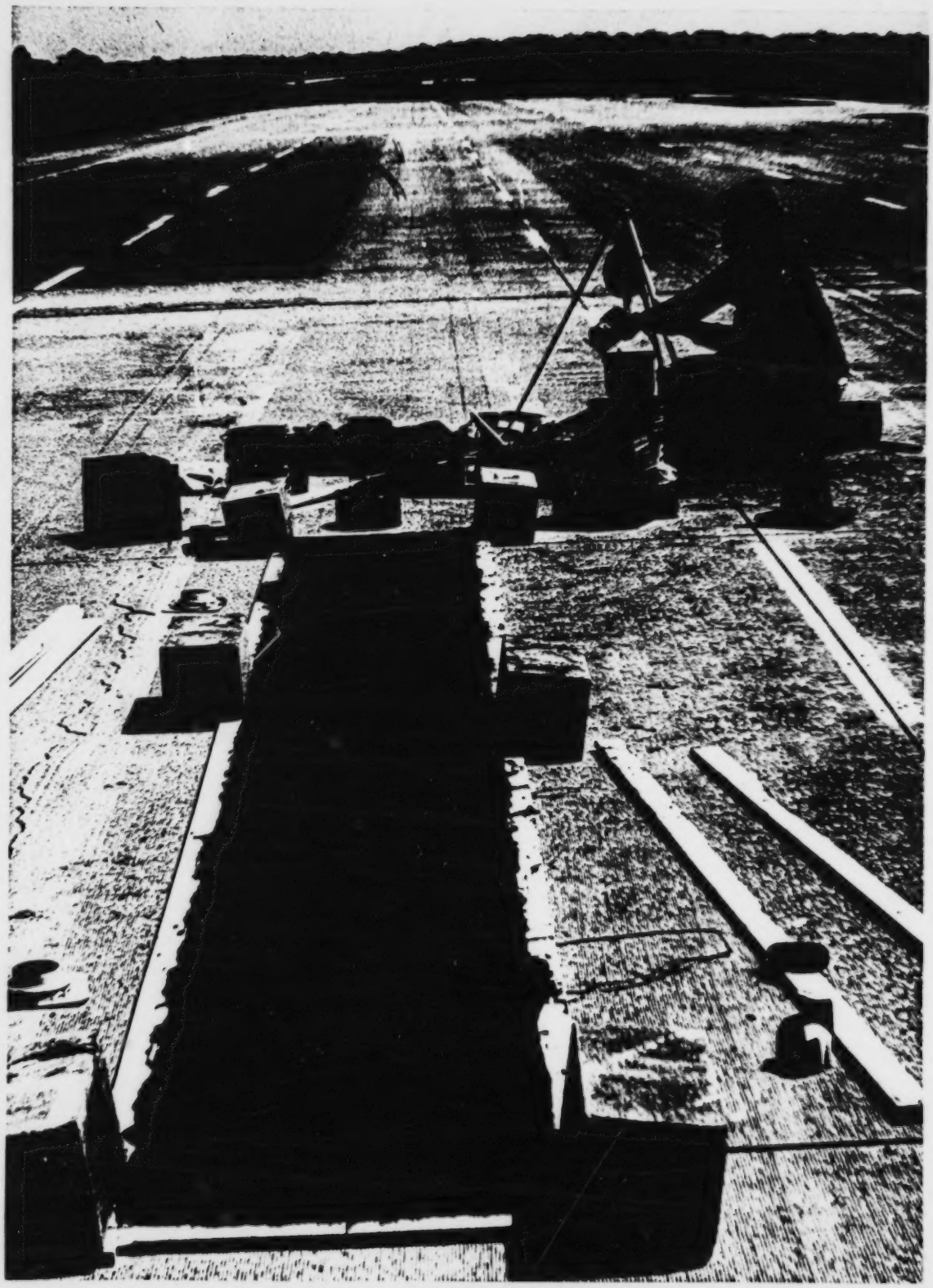

Figure 2. Making Rubber Impression of Pavement.

Figure 3. Replica Asphalt Texture.

Reproduced from best available copy.

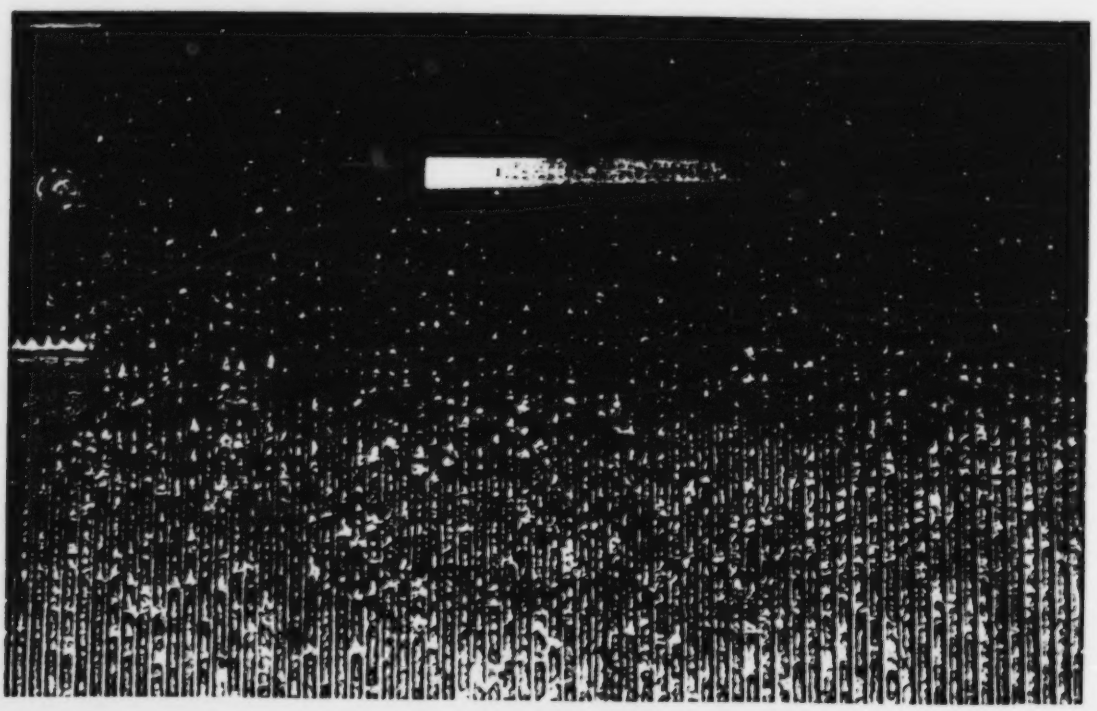

Figure 4. Replica Concrete Texture.

Figure 5. Floating Replica Shell to Roadwheel.

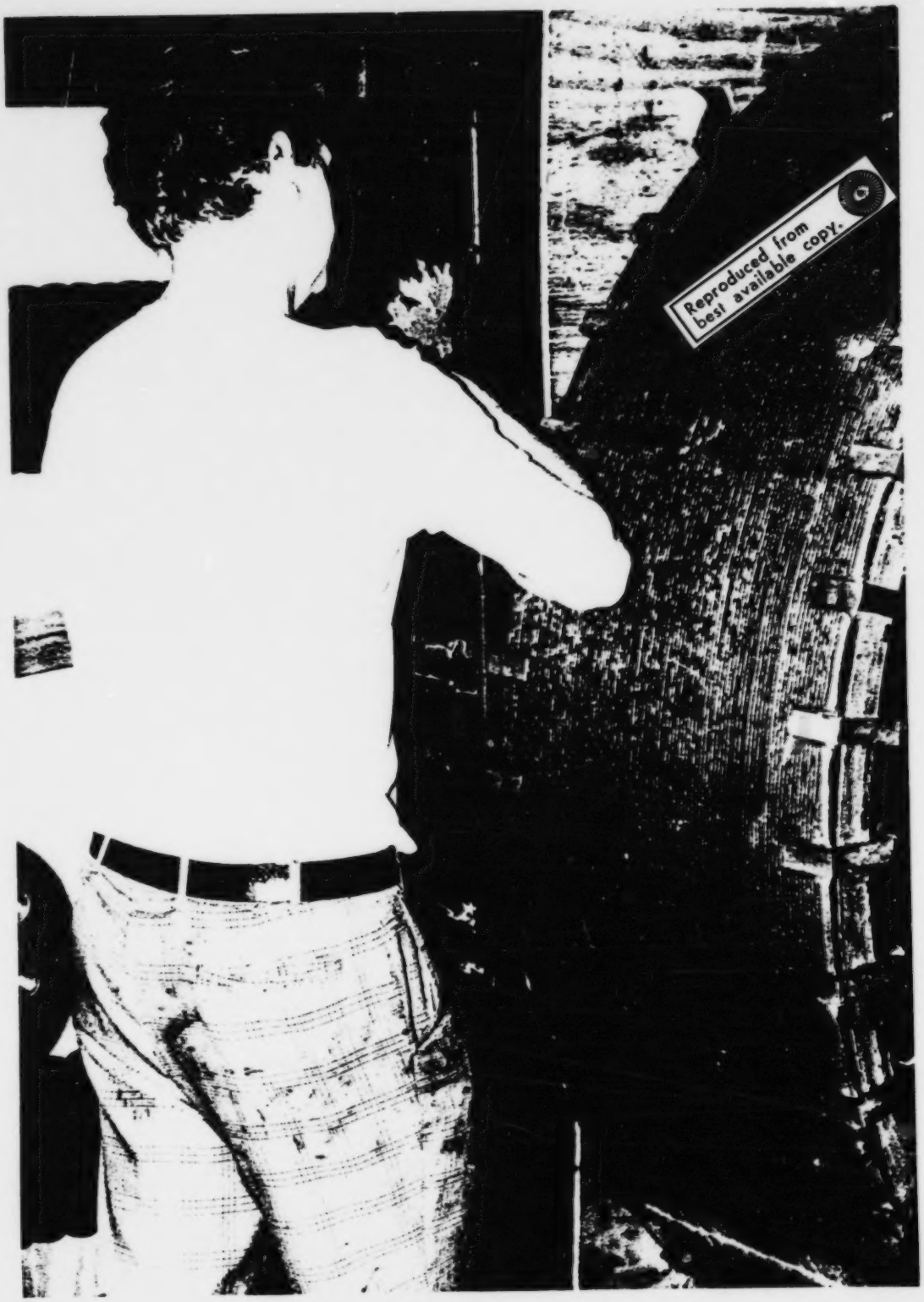

Figure 6. Attachment of Replica Shells Via Clamps.

contact patch opening in the simulated ground plane. A strong air flow was also generated. To correct this, a rigid fiberglass cover plate was fabricated to block the opening. The cover plate provided a channel completely enveloping the clamp path. It eliminated the turbine noise by blocking the associated air flow and by forming an acoustic barrier. Figure 7 shows the interior of the completed facility, including the cover plate, a test tire, and several microphones. Note that the simulated ground plane is the left wall of the chamber; see Figure 1 for orientation.

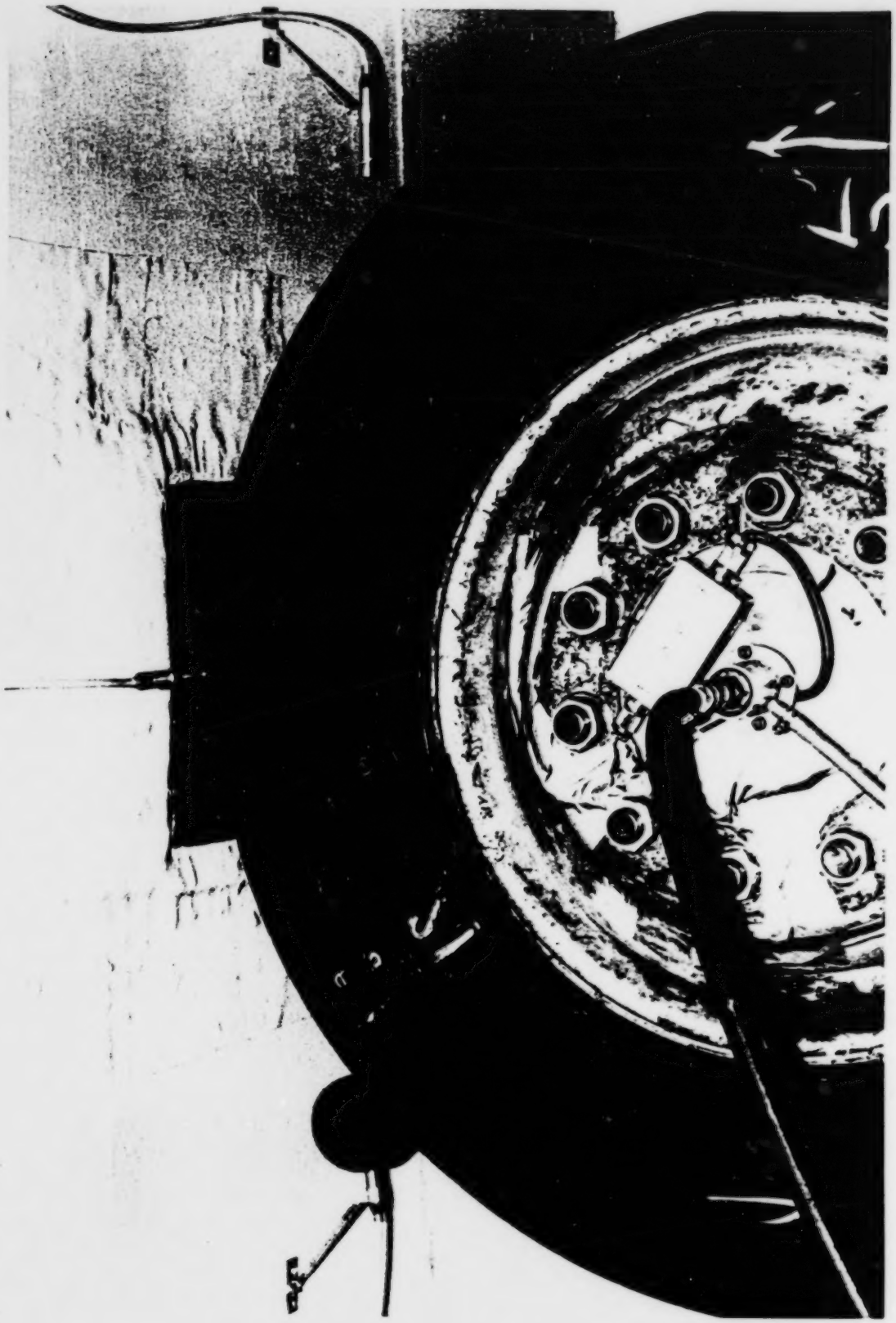

Figure 7. Interior of Acoustic Chamber.

3.0 EXPERIMENTAL PROCEDURES

This chapter describes the experimental procedures that were employed to obtain carcass vibration and near-field sound measurements for a series of four heavy-duty truck tires. The experimental program was carried out in two phases:

- A field measurement phase using a coasting truck on a series of concrete and asphalt road surfaces and on a flat steel plate; and
- An indoor roadwheel phase employing carefully controlled conditions of speed and load on replicas of two of the surfaces investigated in the field measurement.

Section 3.1 contains a description of the test tires that were studied in both phases of the program, Section 3.2 describes the field measurement phase, Section 3.3 describes the roadwheel facility phase, and Section 3.4 describes the data reduction and analysis procedures.

3.1 Test Tires

The four tires tested in this program were those studied in a previous EPA program.[2] They were chosen as being representative of the major carcass and tread designs currently in use on heavy trucks. Table 2 defines the basis for the selection of test tire designs.

To ensure that the tread and carcass variables could be separated, the two bias-ply tires and the two radial-ply tires were each selected from the same manufacturer's brand and type. Except for tread pattern, both tires of each carcass type were identical. Specifications for the four selected tires are given in Table 3. Figure 8 is a photograph of the tires. Figures 9 through 12 show static footprints of each tire.

3.2 Field Measurements

In the field measurement phase of the test program, a rented 1977 White Freightliner, Model 8664T, 10-wheel, cab-over tractor was instrumented at Smithers Scientific Services, Inc., in Ravenna, Ohio, and driven to the Transportation Research Center of Ohio (TRC) in East Liberty, where the coasting measurements were carried out. The tractor was powered by a Cummins 350B diesel engine rated at 350 maximum horsepower at 1900 RPM. The rear axle ratio was 3.70:1.

A block diagram of the instrumentation system used in the coasting tests is shown in Figure 13. Two sets of transducers were employed – the first set fixed on the tire, and the second set fixed on the tractor.

Table 2

Selection of Test Tire Designs

		Rib	Crossbar	Lug
Carcass Design	Bias Ply	X	X	
	Radial Ply	X		X

Table 3

Test Tire Specifications

	#1	#2	#3	#4
MANUFACTURER	B.F. Goodrich	B.F. Goodrich	Firestone	Firestone
TRADE NAME	Milesaver	Milesaver	Power Drive	Transport I
CARCASS	Steel Radial	Steel Radial	Nylon Bias	Nylon Bias
TREAD	Lug	Rib	Crossbar	Rib
PLY RATING	14 Ply	14 Ply	12 Ply	12 Ply
SIZE	11R22.5	11R22.5	11 x 22.5	11 x 22.5

All Tires Are Tubeless.

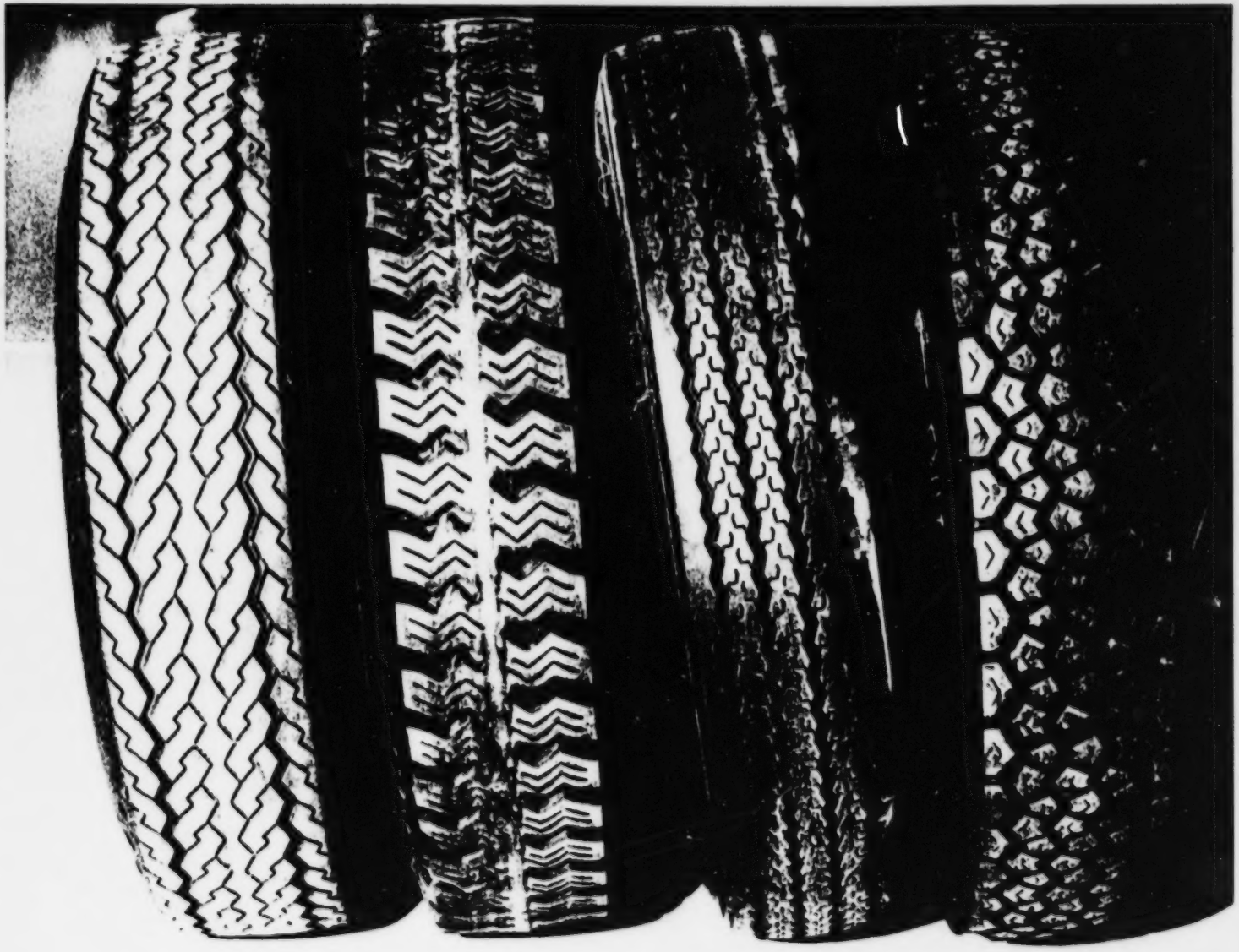

Figure 8. Test Tires. From Left: Bias Rib, Bias Crossbar, Radial Rib, Radial Lug.

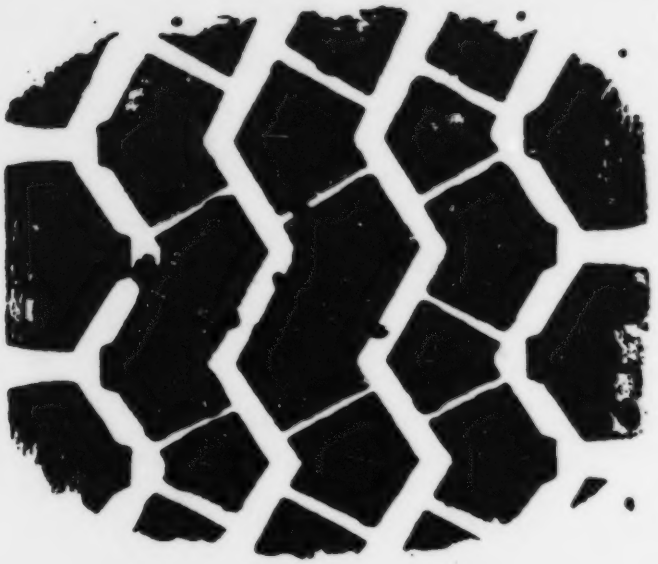

Figure 9. Footprint of Tire #1 — Radial Lug.

Figure 10. Footprint of Tire #2 — Radial Rib.

Figure 11. Footprint of Tire #3 — Bias Crossbar.

Figure 12. Footprint of Tire #4 — Bias Rib.

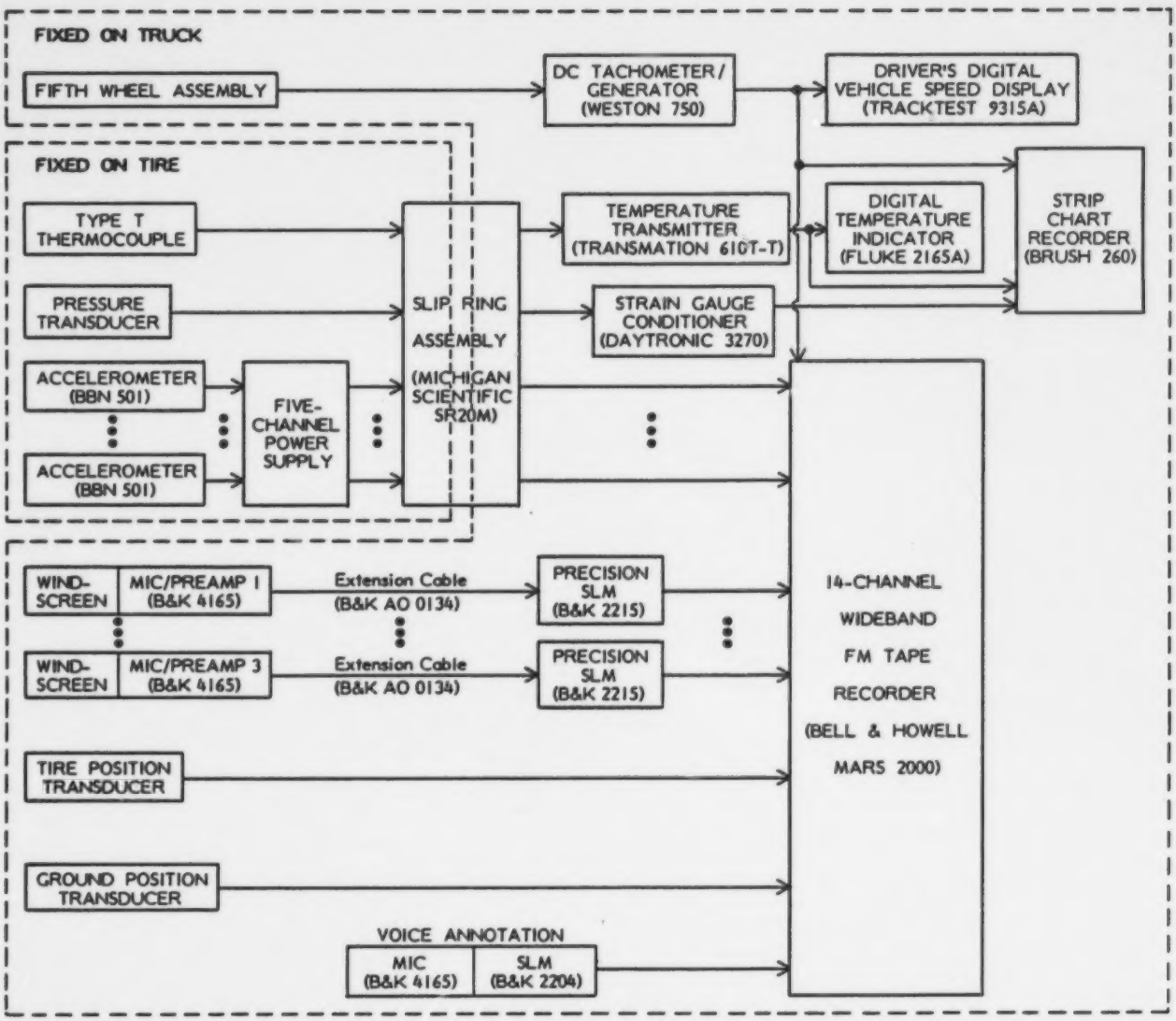

Figure 13. Instrumentation for Outdoor Tests.

The instrumentation fixed on the tire consisted of:

- Five BBN 501 piezoelectric accelerometers mounted inside the tire.
- A five-channel accelerometer power supply mounted on the wheel.
- A tire pressure transducer.
- A Type T thermocouple to measure contained-air temperature.

The outputs of these devices were brought from the rotating tire to the truck body by means of a Michigan Scientific SR20M slip-ring assembly. The slip-ring assembly exhibited no perceptible rippling within the dynamic range of the instrumentation system.

Beneath the truck body and attached to it by various fixtures were the following transducers:

- Three B&K 4165 1/2-inch microphone/preamplifier assemblies in the near sound field of the tire.
- A transducer which marked each tire revolution, thus enabling tire position to be determined.
- A transducer which indicates passage over a fixed point on the ground.

The tire position transducer was a Hall effect switch which produced a pulse when a magnet glued to a tire rim passed by. The ground position transducer was a mechanical micro-switch which closed a circuit when its actuating arm encountered a steel bar placed on the ground, thus producing a voltage pulse. The latter was used to define the two test sections for which molds had been made and to define the position of the steel plate.

The near-field microphone/preamplifier assemblies were mounted on the axle assembly of the truck as follows:

- A microphone one foot to the rear of the contact patch exit and at a height of approximately four inches above the road surface.
- A microphone one foot in front of the contact patch entrance and at a height of approximately four inches above the road surface.
- A microphone one foot to the outside of the tire and approximately six inches above the road surface.

Each of the microphones was enclosed in a windscreen. All mounting brackets and other surfaces near the microphones (e.g., the fuel tanks) were covered with fiberglass batts to reduce acoustic reflections. Figure 14 shows the completed microphone configuration. Also seen in the figure are the slip ring and the accelerometer power supply.

Reproduced from best available copy.

Figure 14. Test Tire on Vehicle, With Microphones in Position.

The microphone/preamplifier assemblies were connected to three B&K 2215 Precision Sound Level Meters which were shock mounted to a board attached to the frame of the tractor. The AC output of each sound level meter was connected to a Bell & Howell Mars 2000 14-channel FM tape recorder, configured to IRIG wideband specifications. The tape recorder all other truck-mounted instrumentation were attached to a four-foot by eight-foot plywood panel which was placed on top of the mattress in the sleeping compartment of the tractor.

Three of the five accelerometers were mounted inside the tire at one circumferential station – one placed at the crown (center of tread area), the second at the shoulder (juncture of tread and sidewall areas), and the third at the sidewall. The other two accelerometers were placed on the crown and sidewall at a station 90 degrees away. The accelerometers were screwed into mounts illustrated in Figure 15. These mounts were developed in Wyle's previous tire study[2] to prevent the accelerometer mounting angle from changing due to lateral force, and also to provide adequate surface area for the inner liner rubber to support the accelerometers. The mounts were assembled and attached to the tire using alpha cynanoacrylic cement. Use of this type of mount permits accelerometers to be removed and reinstalled in exactly the same position.

Accelerometer signals were brought out of the tire through an airtight seal in the rim, and carried through the slip-ring assembly to the FM tape recorder. A battery-powered, five-channel accelerometer power supply was mounted on the side of the rim.

All accelerometer and microphone signals, the tire position and ground position pulses, and a DC voltage proportional to vehicle speed (generated by a fifth wheel assembly) were recorded on the FM tape recorder. A voice annotation of run number and vehicle position relative to the ground position trigger was recorded. DC signals proportional to vehicle speed, tire contained-air temperature, and tire pressure were recorded on a strip-chart recorder. A digital display of the vehicle speed was provided to the driver. A Nicolet 444A FFT spectrum analyzer was used to monitor transducer signals during instrumentation checkout, and to inspect recorded data after each set of runs.

For the coasting tests all but two of the eight rear tires of the tractor were removed. The forward tire on the left (driver's) side of the vehicle was the test tire; that on the right side of the vehicle was a rib tire of similar size, as were the front two tires. Figure 16 shows the vehicle configuration during a typical coasting test on the unsealed asphalt surface. Figure 17 shows the vehicle approaching the flat steel plate. Note the ground position switch arm on the front of the vehicle about to come into contact with the steel bar on the ground.

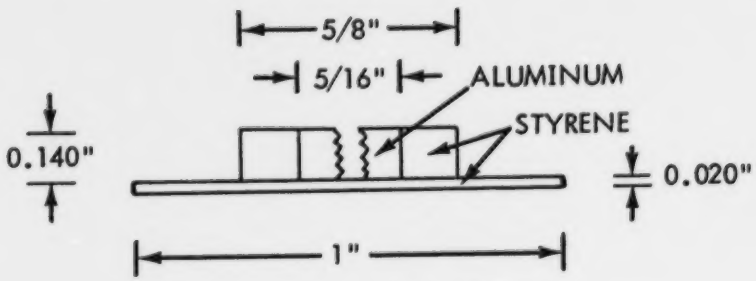

Figure 15. Accelerometer Mount Design.

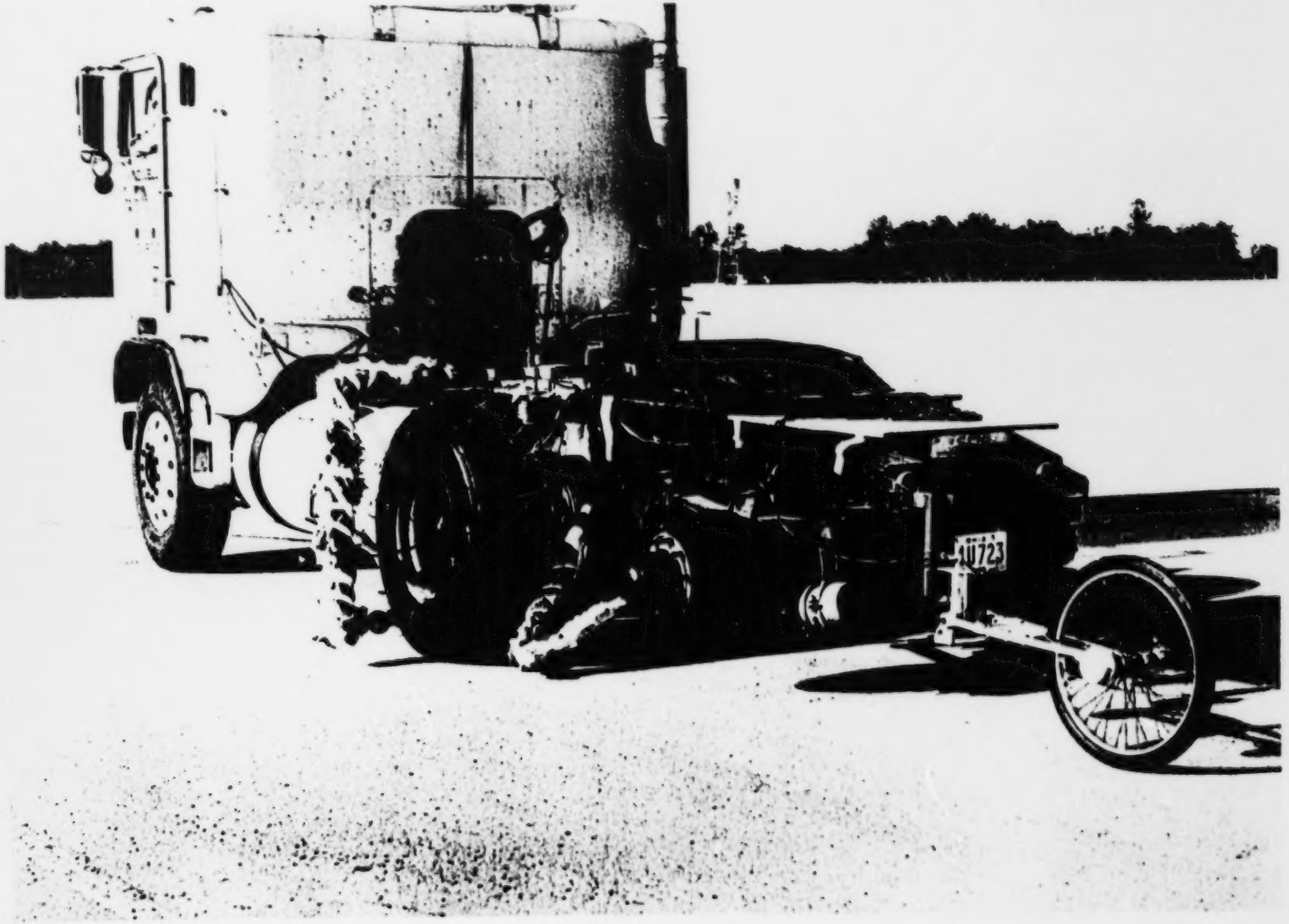

Figure 16. Test Vehicle on VDA.

Figure 17. Test Vehicle Approaching Flat Steel Plate.

Coasting tests were carried out at two different facilities at TRC. Tests on concrete surfaces and on the flat steel plate were done on the skid pad; those on asphalt surfaces were done in the vehicle dynamics area.

The skid pad, illustrated in Figure 18, is a test facility which is utilized primarily for the evaluation of tire and brake systems. The overall dimensions of the pad are 9,000 feet by 84 feet with turnaround loops on the north and south ends. The acceleration/deceleration lanes at each end are 3,280 feet in length. A test area of 210,000 square feet is situated in the center of the skid pad, containing several test pads with varying surface textures. Skid numbers in this area range from 30 (wet) to 80 (dry). The skid pad is paved with Portland cement. The load capacity of the skid pad is 36,000 pounds maximum single-axle weight and 48,000 pounds maximum tandem-axle weight.

The vehicle dynamics area (VDA), illustrated in Figure 19, is an asphalt pad which measures 1,200 feet by 1,800 feet, covering 50 acres. The test surface has a one-percent downward slope from north to south. There is no cross-slope. The VDA is bordered on the north and south ends with loops which allow rapid entry and exit from the test pad. The composition of the pad and turnaround loops is bituminous concrete. The facility has provisions for wet and dry testing. Nominal skid numbers range from 75 to 80 on dry pavement, and 60 to 65 on wet pavement. Sealed asphalt areas are available for those desiring lower skid numbers. The load capacity of the pad and loops is 36,000 pounds maximum single-axle weight, and 48,000 pounds tandem-axle weight.

Coasting tests on six different surfaces were carried out at these two facilities. Figures 20 through 25 are photographs of the surfaces; included in each photograph is a 25-cent piece (0.96-inch diameter) as a size reference. The surfaces were:

- Surface A1 – Unsealed Asphalt (Figure 20) consisted of fine topcoat (Ohio 404*) over a coarser underlayment (Ohio 402*). This surface is typical of unsealed asphalt roadways.
- Surface A2 – Sealed Asphalt (Figure 21) was similar to Surface A1 except that it has been sealed with two coats of Jennite sealer followed by two coats of X-10 sealer. Jennite is a coal-tar emulsion sealer containing filler; X-10 is a similar emulsion containing no filler. This surface is smoother than those found on most asphalt roadways.

---

* See Appendix A for characteristics of these surfaces.

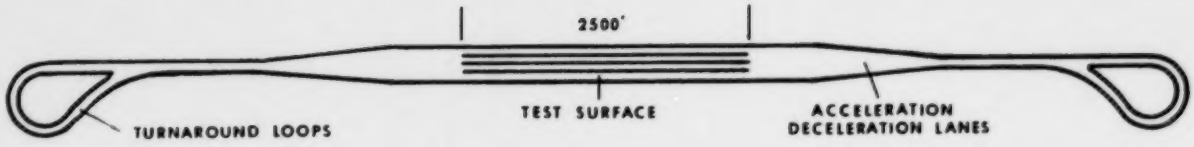

Figure 18. Skid Pad at Ohio TRC.

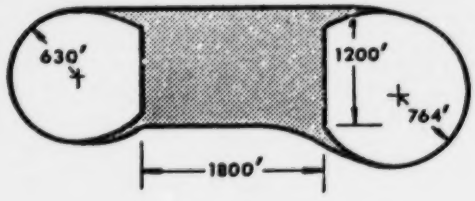

Figure 19. Vehicle Dynamics Area at TRC.

Figure 20. Unsealed Asphalt (A1).

Reproduced from best available copy.

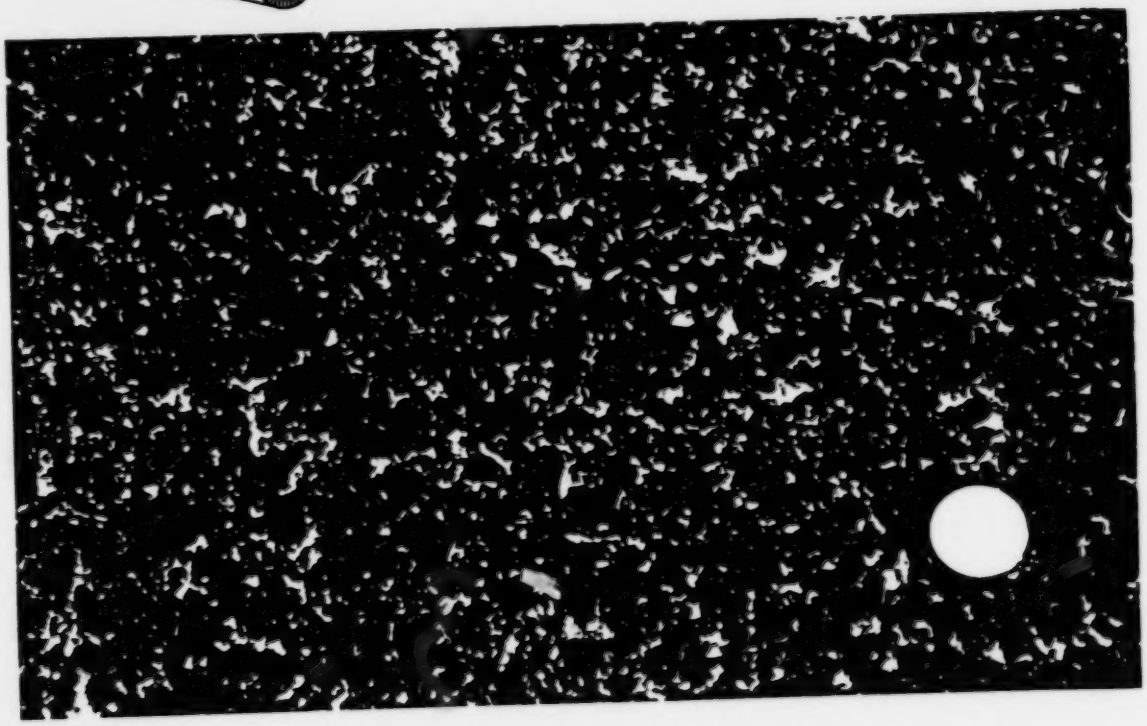

Figure 21. Sealed Asphalt (A2).

- Surface C1 – "Medium" Concrete (Figure 22) consisted of broomed Portland cement concrete with grooves parallel to the direction of travel. This surface is similar to those found on interstate highways, and is referred to in TRC documentation as "Interstate Concrete".
- Surface C2 – "Smooth" Concrete (Figure 23) consisted of smooth trowled and polished Portland cement concrete. This surface is considerably smoother than those typically found on highways.
- Surface C3 – "Rough" Concrete (Figure 24) consisted of coarse broomed Portland cement concrete. This surface is somewhat rougher and more irregular than Surface C1.
- Surface S – Steel Plate (Figure 25) consisted of a 2-foot by 22-foot steel plate bolted to one of the concrete skid pad lanes. The approach end of the steel plate was beveled so that a smooth transition occurred between the concrete and the plate.

Rubber molds were cast of concrete Surface C1 and asphalt Surface A1 for use in preparing replica roadwheel surfaces, as described in Section 2.

The sequence for each coasting test was as follows:

- During several trial runs, the driver determined the acceleration profile required to coast over the pavement test section at the desired speed. The trial runs provided a warm-up.
- Driver accelerated vehicle as needed, then disengaged clutch and turned off engine.
- Technician turned on tape recorder and strip-chart recorder.
- Technician annotated run number and counted down (on voice annotation recording) vehicle position relative to test section.
- After vehicle had passed test section, driver turned on engine and reengaged clutch.

For each coasting test, the tire was loaded to 75 percent of its maximum rated load and inflated to its maximum rated pressure.

Table 4 shows the minimum number of coastings carried out for each tire. For all surfaces except the steel plate, coastings were done in both lane directions. Since only one end of the steel plate was beveled, all coastings on this plate were done in the same direction. No 50 mph coastings were done on the steel plate since it could not be reliably traversed at that speed (the width of the plate between the hold-down bolts was only 22 inches).

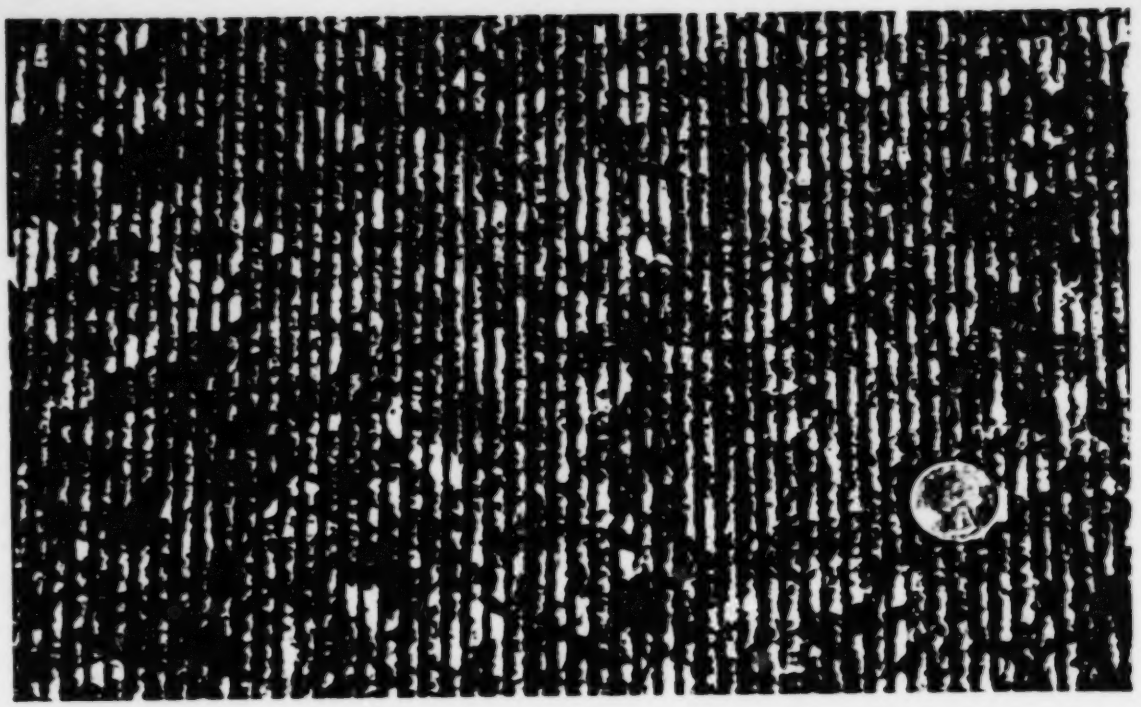

Figure 22. Medium ("Interstate") Concrete (C1).

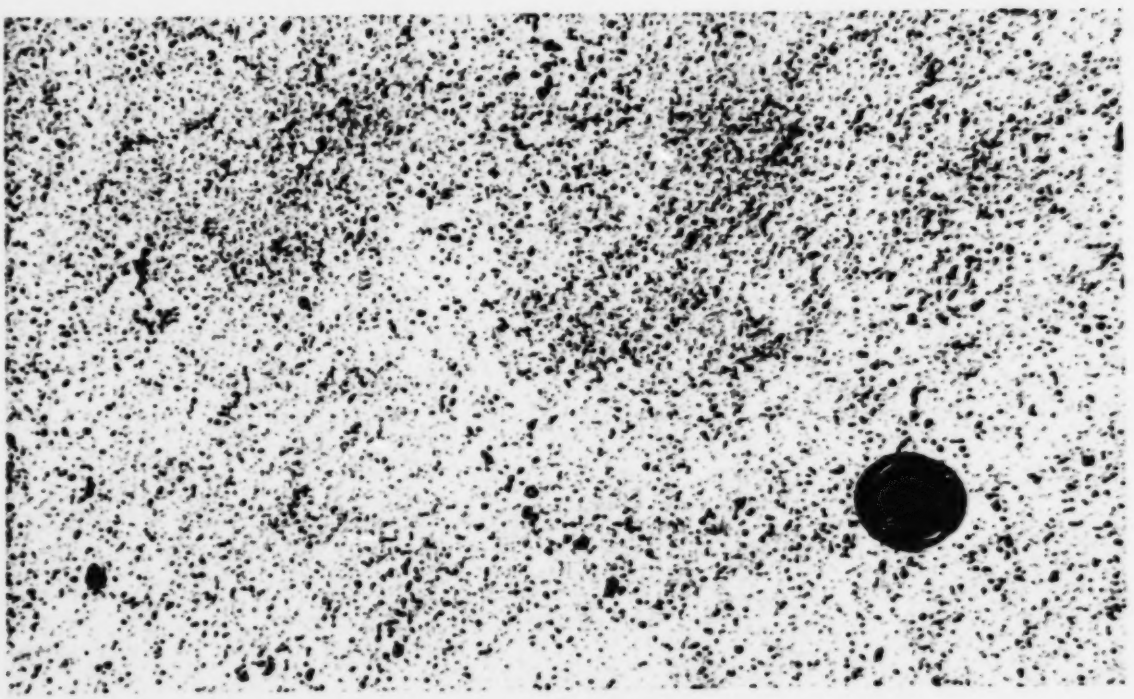

Figure 23. Smooth Concrete (C2).

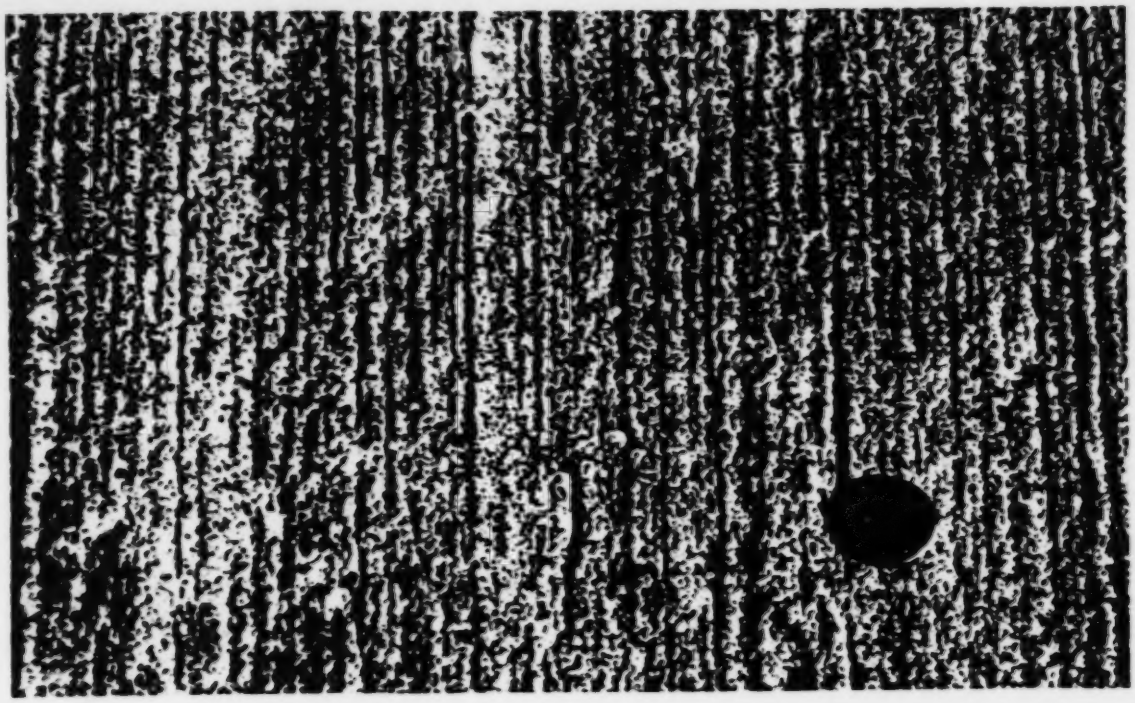

Figure 24. Rough Concrete (C3).

Reproduced from
best available copy.

Figure 25. Steel Plate (S).

Table 4

Coastby Test Matrix For Each Tire
(Number Indicates Minimum Number of
Coastbys Carried Out)

Surface	Vehicle Speed (mph)		
	20	35	50
C1	2	4	2
C2		4	
C3		4	
A1	2	4	2
A2		4	
S	2	4	

3.3 Roadwheel Measurements

A series of measurements were conducted on the same four test tires, using the facility described in detail in Section 2.0. An instrumentation system similar to that used for the field measurements was assembled. Figure 26 is a schematic of the system. Differences in instrumentation, other than model types indicated in Figures 13 and 26, are:

- Infrared LED/phototransistor pairs, triggered by reflective tape on the tire and roadwheel, provided rotational reference pulses.
- Roadwheel position, rather than vehicle reference mark, was recorded.
- Five acoustic channels were available. Three were used, corresponding to the outdoor measurement points.
- Tire pressure could be regulated as well as measured.
- Ambient temperature was recorded.
- The Nicolet 444A analyzer and a pen plotter were wired into the system for on-line examination of data, as well as system checkout.

Figure 27 shows the recording equipment arranged at the roadwheel machine. The optical sensor for roadwheel position index is seen adjacent to the axle shaft, lower center.

Data were collected for a baseline and warm-up test matrix similar to that used in the previous roadwheel test program.[2] The 27-point matrix previously used consists of all combinations of:

- 20, 35, and 50 mph;
- 50, 75, and 100 percent rated load;
- Rated inflation pressure, and rated pressure $\pm$15 psi.

This matrix permits full evaluation of the parametric behavior of tire noise as well as comparison with the 75 percent load-rated pressure data taken in the outdoor field tests. Due to high temperature conditions encountered in the chamber,* the conditions including both low pressure and high load were deleted. A 24-point test matrix was thus employed. Before each test sequence, the tires were warmed to stable conditions, based on the warm-up data collected for these tires in the previous program.[2]

---

* Outside air was used to cool the chamber between runs. Seasonal temperatures during October, when these replica pavement tests were performed, were not as favorable as during January when the smooth steel roadwheel tests were conducted.

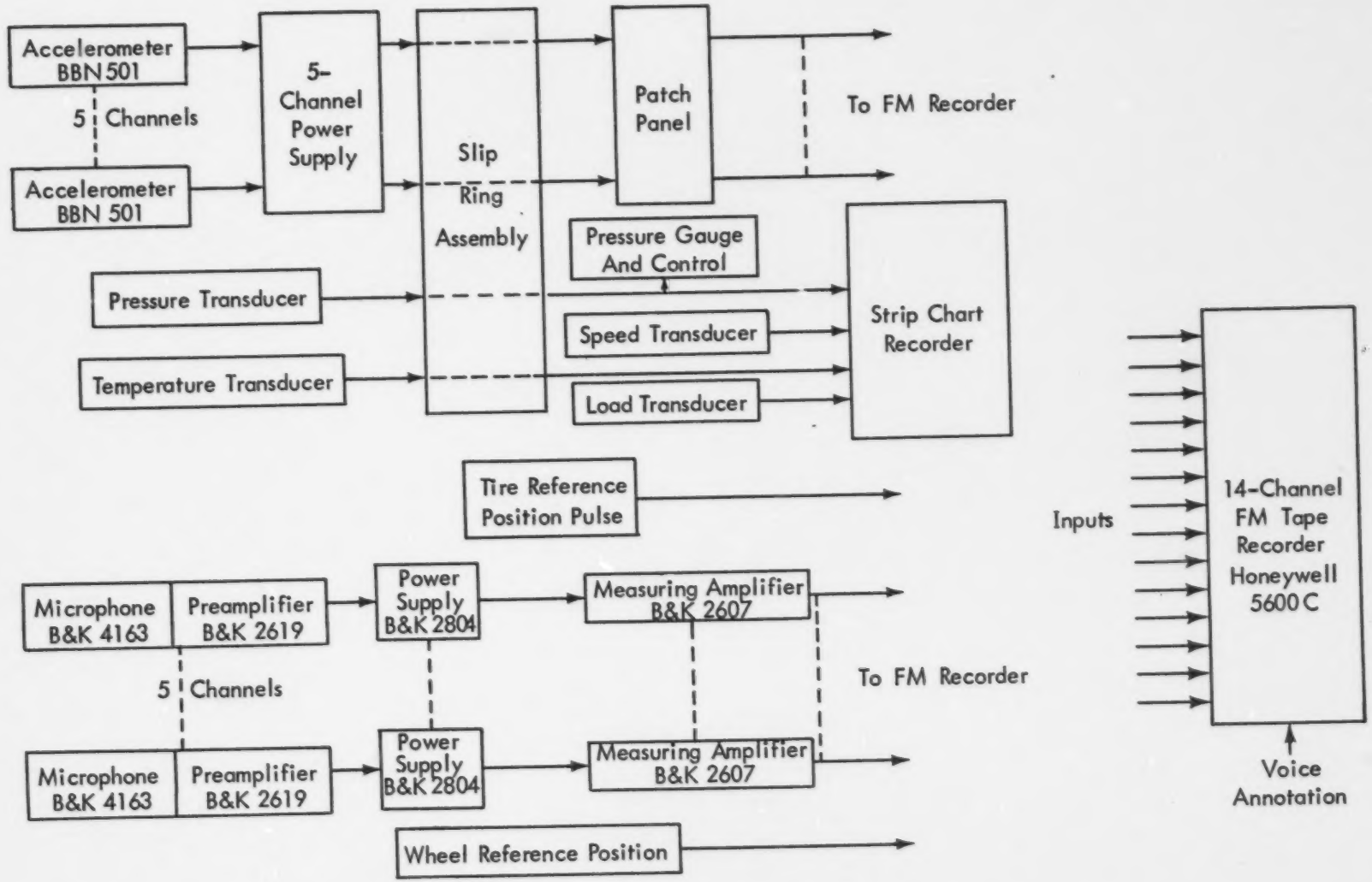

Figure 22. Instrumentation for Roadwheel Measurements.

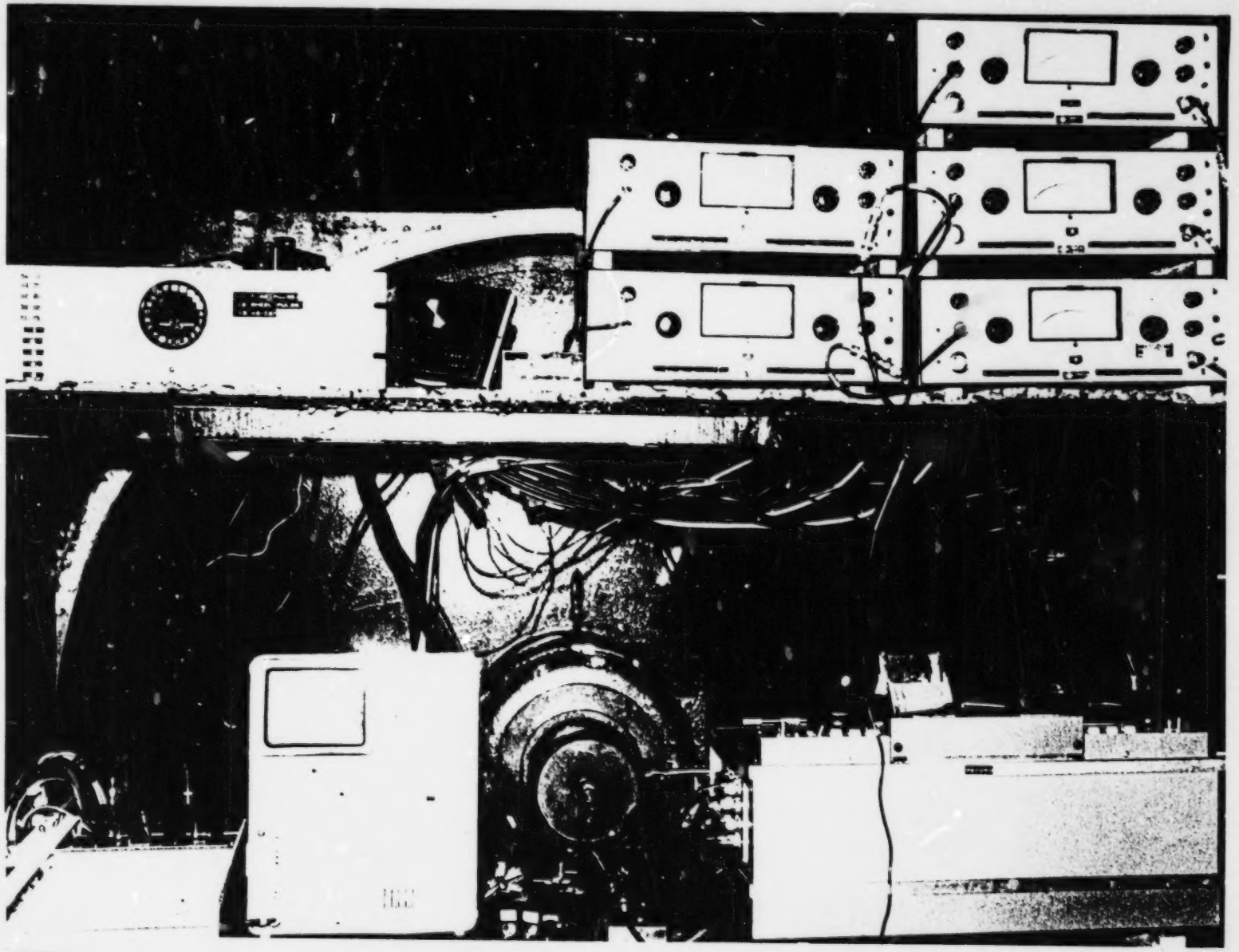

Reproduced from best available copy.

Figure 27. Instrumentation System in Place at Roadwheel.

3.4 Data Reduction and Analysis

For data reduction and analysis, a data processing system consisting of a Nicolet 444A FFT spectrum analyzer interfaced to a Digital Equipment PDP 11V03 minicomputer was used. The PDP-11 uses an LSI-11 CPU with 32K words of memory. The system also includes a dual floppy disc drive and an LA-36 terminal. The interface is used to control the analyzer from the computer and to pass data from the analyzer to the computer for processing and storage and from the computer to the analyzer for analysis and display. An X-Y plotter, connected to the spectrum analyzer, is used to obtain permanent plots of temporal and spectral records.

A block diagram of this system is shown in Figure 28. The same 14-channel tape recorders as were used to collect the data were used to play back the analog signals. These signals were digitized and transformed to spectra using the Nicolet analyzer. The digitized spectral levels (generally averaged over a number of samples) were then stored on floppy discs. Overall and A-weighted sound pressure levels were calculated from the spectra. The analysis system also permitted storage and processing of selected time samples. The pulse counter/time shifter permitted sampling by the analyzer to be synchronized with the tire or wheel pulse. A continuously variable time delay could be applied, permitting analysis of any desired time window. The counter feature provided for sampling and holding the N'th ($1 \leq N \leq 15$, switch-selectable) synchronized sample following a data start signal. A suitable data start signal was included on the voice track. This last feature permitted comparison of successive revolutions of the tire and/or roadwheel.

The analysis performed, and presented in Section 4, includes:

- A-weighted levels for all outdoor surfaces and test conditions.
- Comparison of A-weighted levels between the real and replica surfaces A1 and C1, and also data for the same tires on a smooth steel roadwheel.
- Comparison of selected spectra and time histories for the comparison of real texture, replica texture, and smooth steel.

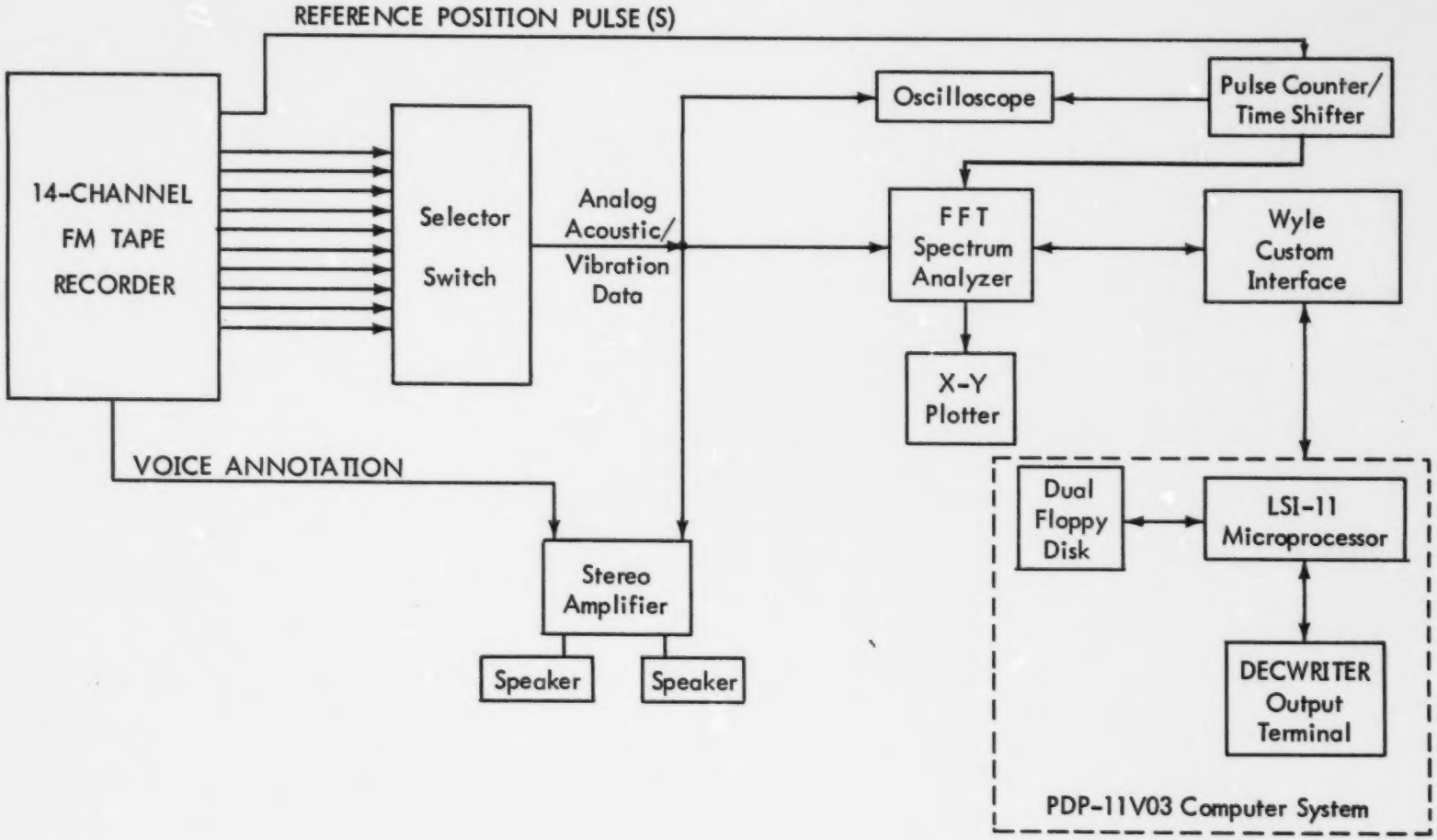

Figure 23. Instrumentation for Data Reduction.

4.0 EXPERIMENTAL RESULTS

This chapter describes the experimental results that were obtained from the two measurement programs described in Chapter 3.

Section 4.1 presents a detailed analysis of A-weighted sound levels. Sections 4.1.1 and 4.1.2 describe the results of the field measurements, the former discussing the effect of carcass and tread design on near-field sound levels, and the latter discussing the effect of roadway surface on these levels. These sections are essentially a data report, and the conclusions cannot necessarily be generalized beyond the tires and surfaces tested. Section 4.1.3 compares the results of the roadwheel measurements with those of the field measurements. The objective of this section is to evaluate the realism of the pavement simulation technique. Previously collected data from a smooth steel roadwheel[2] are included in the comparison. Section 4.1.4 compares flat steel plate and smooth roadwheel data, to evaluate the effect of curvature.

Section 4.2 presents a discussion of the effect of real and simulated texture on spectra and time signatures.

4.1 Analysis of A-Weighted Sound Levels

4.1.1 Effects of Carcass and Tread Design

Figure 29 shows the measured A-weighted sound level at each of the three microphone positions as a function of vehicle speed and tire type on the interstate concrete surface (C1). Figure 29, and following figures, show data for each microphone position arranged around a schematic of the tire. Direction of travel of the tire is shown. Figure 30 shows a similar set of curves for the unsealed asphalt surface (A1). Table 5 summarizes the identity of the noisiest and quietest tire type and indicates the sound level range for all microphone positions, vehicle speeds, and both surfaces. In this summary, tire types having level differences of one dB or less have been considered to have equivalent levels.

The following conclusions can be reached from these data:

- The bias-ply crossbar tire is generally (one exception) the noisiest tire at all speeds and microphone positions on both surfaces.
- The bias-ply crossbar tire is always the noisiest tire at all speeds and on both surfaces at the front and rear microphone positions.
- The radial-rib tire is always the quietest tire at all speeds and microphone positions on both surfaces.

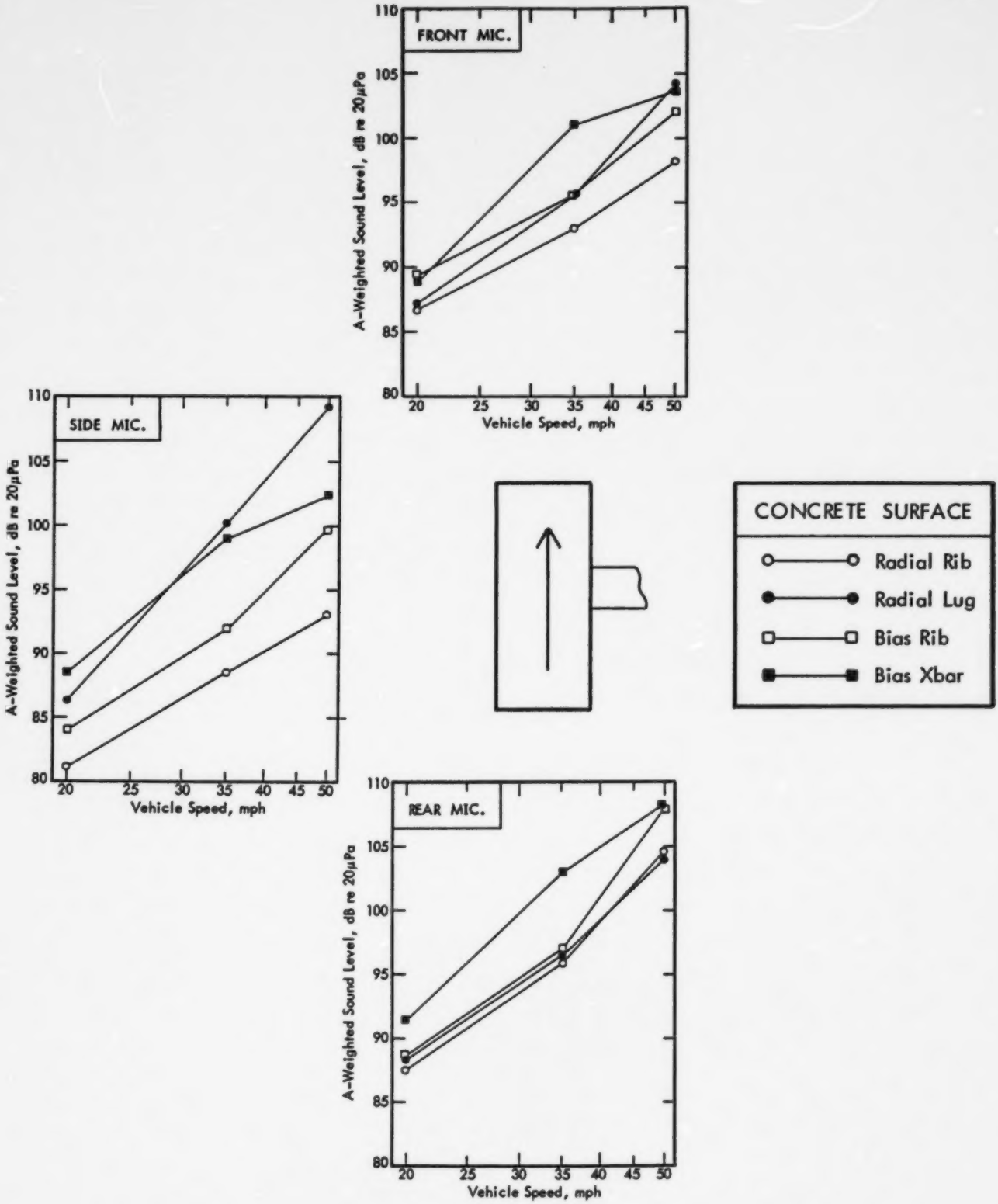

Figure 29. A-Weighted Sound Level Versus Vehicle Speed as a Function of Tire Type for Concrete Surface (C1).

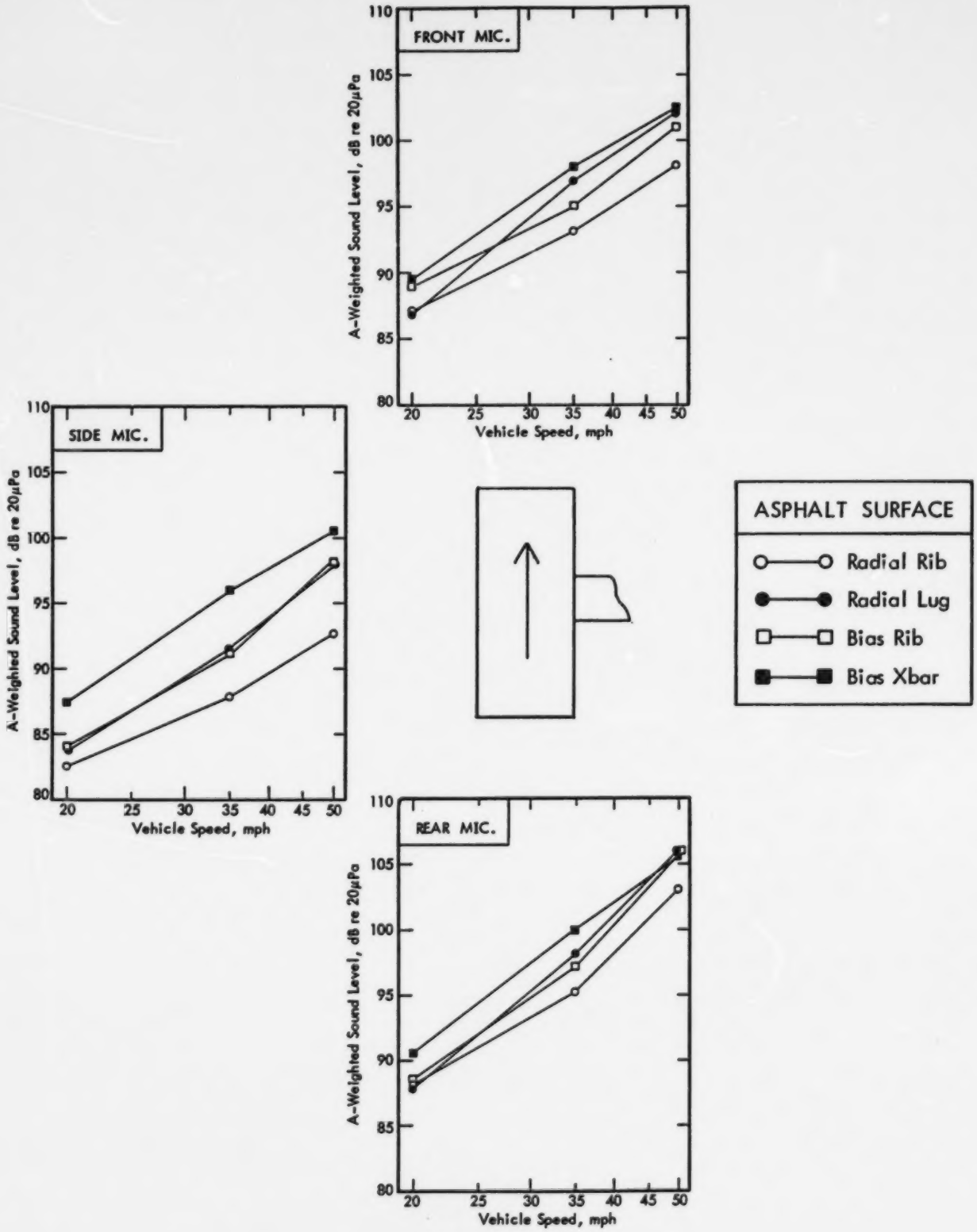

Figure 30. A-Weighted Sound Level Versus Vehicle Speed as a Function of Tire Type for Asphalt Surface (A1).

Table 5

Summary of Noisiest and Quietest Tire Types

Vehicle Speed, mph	Micro-phone	CONCRETE SURFACE (C1)			ASPHALT SURFACE (A1)		
		Noisiest	Quietest	Level Spread, dB*	Noisiest	Quietest	Level Spread, dB
20	Front	BX & BR	RR & RL	3	BX & BR	RR & RL	2
	Rear	BX	RR & RL	4	BX	RR & RL	2
	Side	BX	RR	8	BX	RR	5
35	Front	BX	RR	8	BX	RR	5
	Rear	BX	RR & RL	7	BX	RR	5
	Side	BX & RL	RR	11	BX	RR	8
50	Front	BX & RL	RR	6	BX & RL	RR	4
	Rear	BX & BR	RR & RL	4	BX, BR & RL	RR	3
	Side	RL	RR	16	BX	RR	8

Tire Code:

RR – Radial Rib , RL – Radial Lug

BR – Bias Rib , BX – Bias Crossbar

* Difference between noisiest and quietest tires, as shown in figures.

4.1.2 Effects of Roadway Surface

Figures 31 through 34 show the measured A-weighted sound levels at each of the three microphone positions as a function of vehicle speed and roadway surface type for each of the four tires tested. Table 6 summarizes the identity of the noisiest and quietest roadway surfaces and indicates the sound level range for all microphone positions, vehicle speeds, and tire types. In this summary, roadway surfaces having level differences of one dB or less have been considered to have equivalent levels.

The following conclusions can be reached from this data:

- Smooth surfaces (sealed asphalt and smooth concrete) are generally (two exceptions) the noisiest at all speeds and microphone positions for all tires.
- The smooth concrete surface is generally (two exceptions) the noisiest at 50 mph and all microphone positions for all tires.
- Rough surfaces (asphalt and rough concrete) are generally (two exceptions) the quietest at all speeds and microphone positions for all tires.
- The asphalt surface is generally (two exceptions) the quietest at 50 mph and all microphone positions for all tires.

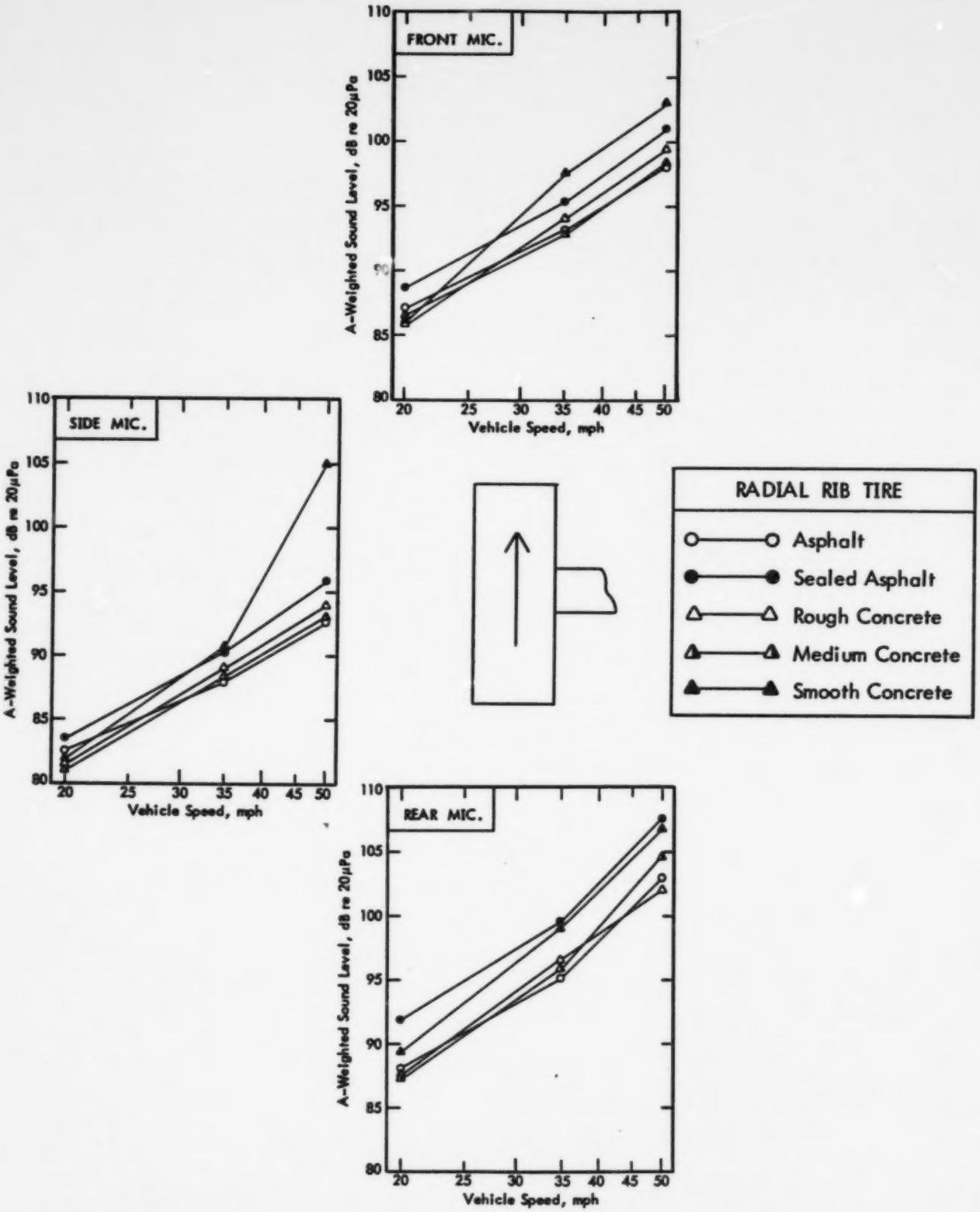

Figure 31. A-Weighted Sound Level Versus Vehicle Speed as a Function of Roadway Surface for Radial Rib Tire.

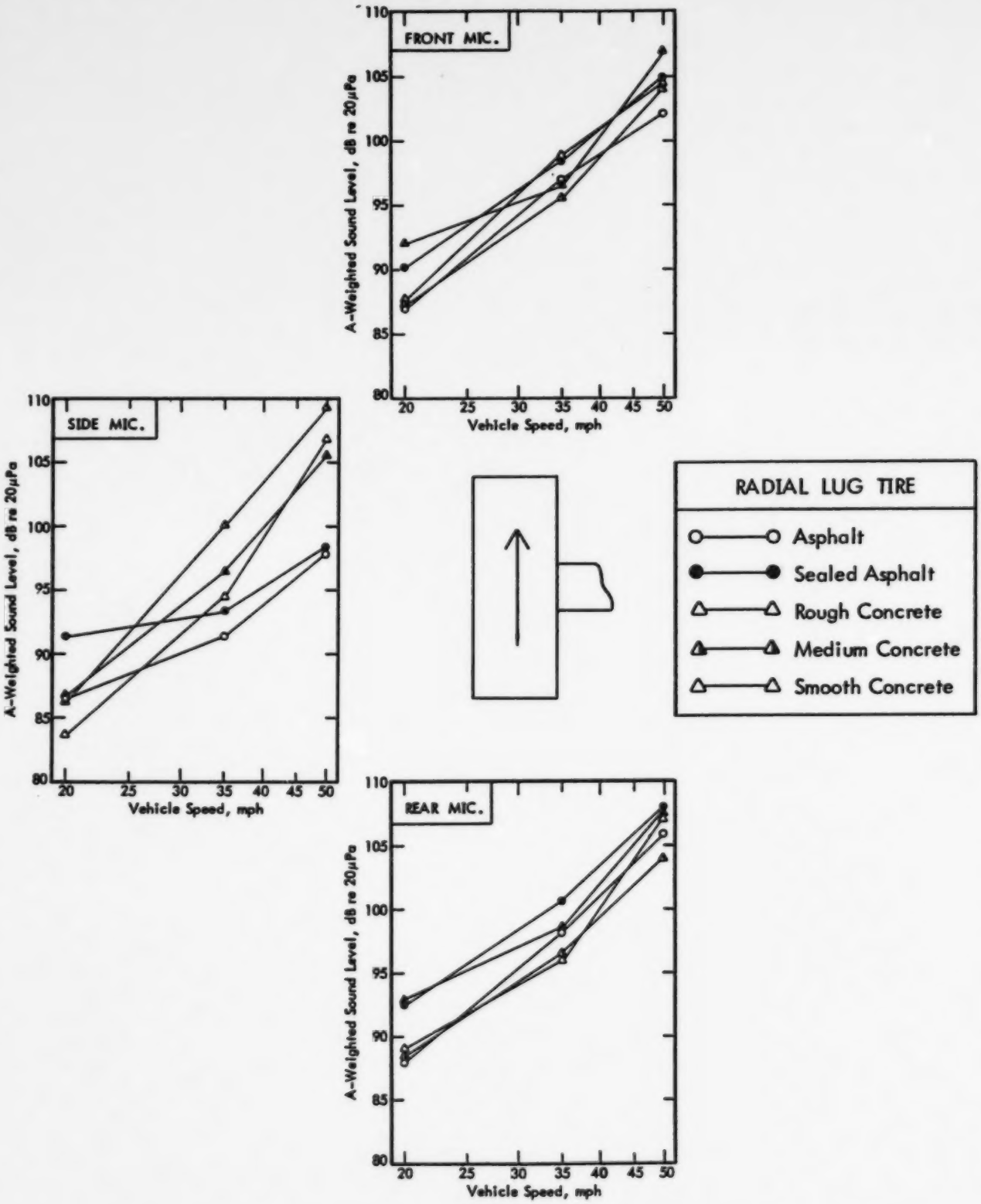

Figure 32. A-Weighted Sound Level Versus Vehicle Speed as a Function of Roadway Surface for Radial Lug Tire.

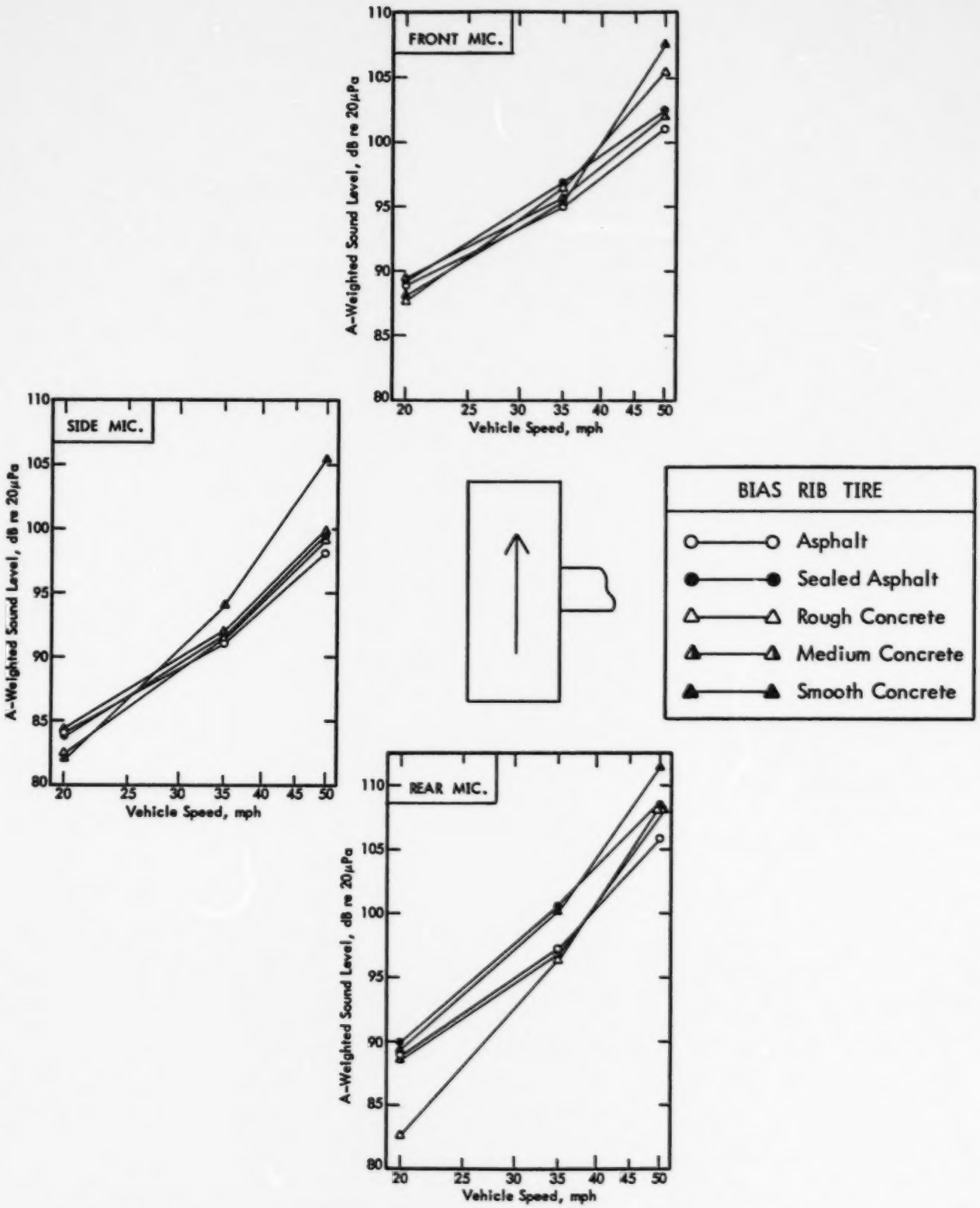

Figure 33. A-Weighted Sound Level Versus Vehicle Speed as a Function of Roadway Surface for Bias Rib Tire.

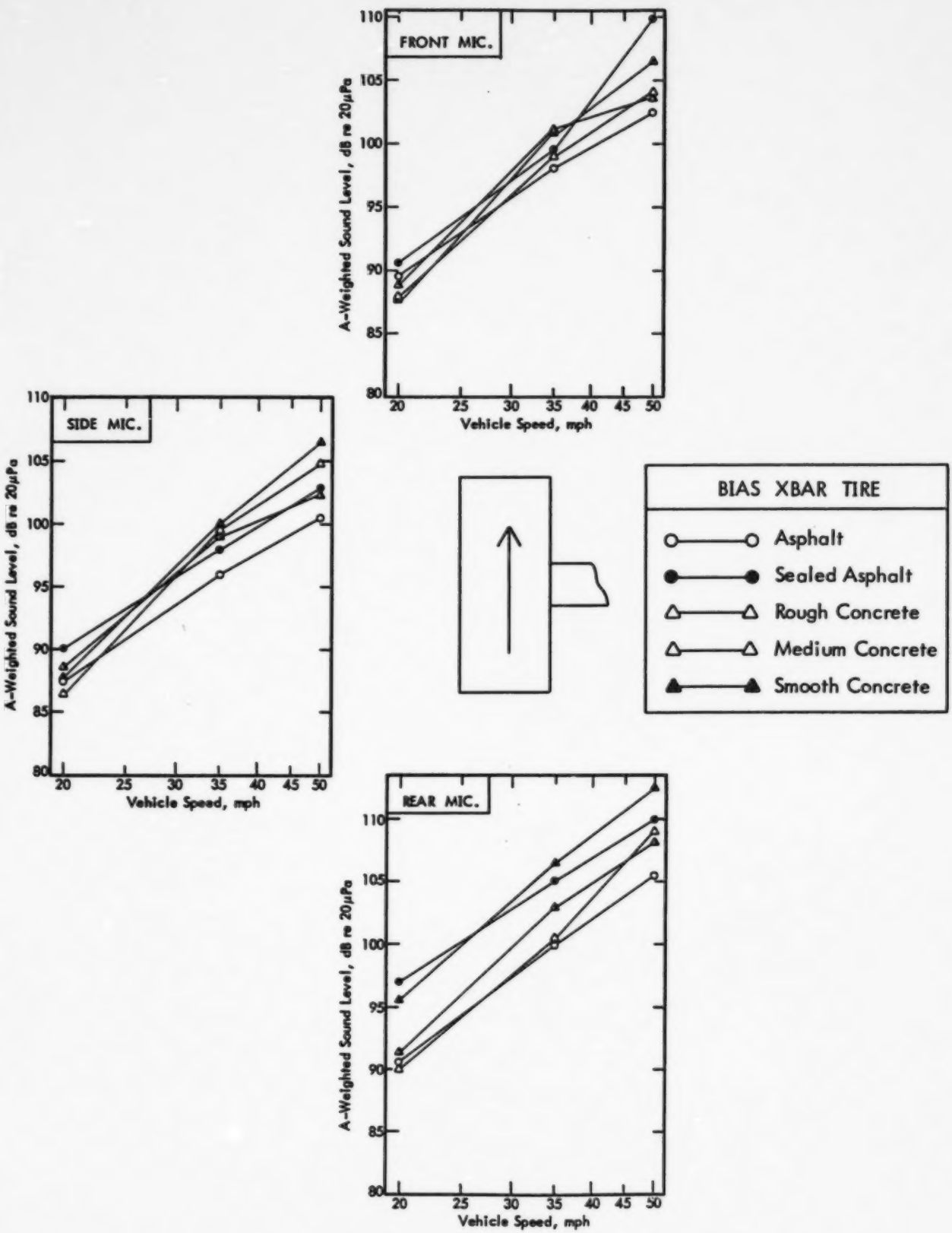

Figure 34. A-Weighted Sound Level Versus Vehicle Speed as a Function of Roadway Surface for Bias Crossbar Tire

Table 6

Summary of Noisiest and Quietest Roadway Surfaces

		RADIAL RIB TIRE			RADIAL LUG TIRE		
Vehicle Speed, mph	Micro-phone	Noisiest	Quietest	Level Spread, dB	Noisiest	Quietest	Level Spread, dB
20	Front	SA	RC & SC	2	SC	A, RC, MC	5
	Rear	SA	RC & MC	4	SA & SC	A & MC	5
	Side	SA	RC & MC	2	SA	RC	8
35	Front	SC	A & MC	4	SA & RC	MC	4
	Rear	SA & SC	A	4	SA	RC & MC	4
	Side	SA & SC	A & MC	2	MC	A	8
50	Front	SC	A & MC	5	SC	A	5
	Rear	SA & SC	RC	6	SA, RC, & SC	MC	4
	Side	SC	A & MC	12	MC	A & SA	12

		BIAS RIB TIRE			BIAS XBAR TIRE		
Vehicle Speed, mph	Micro-phone	Noisiest	Quietest	Level Spread, dB	Noisiest	Quietest	Level Spread, dB
20	Front	RC & SC	A, SA, MC	2	SA	RC & SC	3
	Rear	SA & SC	RC	8	SA	A & RC	7
	Side	A, SA, RC	RC & SC	2	SA	RC	4
35	Front	SA & RC	A, MC, SC	2	MC & SC	A	3
	Rear	SA & SC	A, RC, MC	4	SC	A & RC	6
	Side	SC	A & RC	3	SC & RC	A	4
50	Front	SC	A	6	SA	A	7
	Rear	SC	A	6	SC	A	7
	Side	SC	A	8	SC	A	6

Roadway Surface Code:

A – Asphalt (A1), SA – Sealed Asphalt (A2)

RC – Rough Concrete (C3), MC – Medium Concrete (C1), SC – Smooth Concrete (C2)

4.1.3 Comparison of Roadway and Roadwheel Results

Figures 35 through 38 show the measured A-weighted sound levels at each of the three microphone positions as a function of vehicle speed and surface type (roadway, replica roadwheel, steel roadwheel) for each of the four tires tested. Also indicated on the figures are the least squares best-fit of the form $L_A = C_1 \log_{10} V + C_2$. Each figure consists of two parts: the (a) part refers to concrete roadway and replica roadwheel surfaces; the (b) part refers to asphalt roadway and replica roadwheel surfaces.

In general, the replica roadwheel levels more closely approximate the roadway levels than do the steel roadwheel levels. This can be better seen in Figure 39, which shows (for all tires and microphone positions, and for both roadway types) the A-weighted sound level on the roadway as a function of the A-weighted sound level on the replica roadwheel and as a function of the A-weighted sound level on the steel roadwheel. Each plot shows the best-fit linear relation between roadway data and roadwheel data. The fit for the replica roadwheel has a smaller standard error of estimate, σ_L, a larger correlation coefficient, r, and a slope more nearly unity than does the fit for the steel roadwheel.

Figure 40 shows similar plots in which the best unit-slope linear relation between roadway data and roadwheel data are shown. Again, the replica roadwheel more closely models the roadway data than does the steel roadwheel data. As seen in Figure 41, the difference between replica roadwheel and steel roadwheel is even more pronounced if only the data from the rear microphone (that at which the sound levels are generally the highest) are considered. It is therefore concluded that, with regard to A-weighted sound levels, the replica surfaces provide a very good simulation of the real surfaces, and are superior to a plain steel surface.

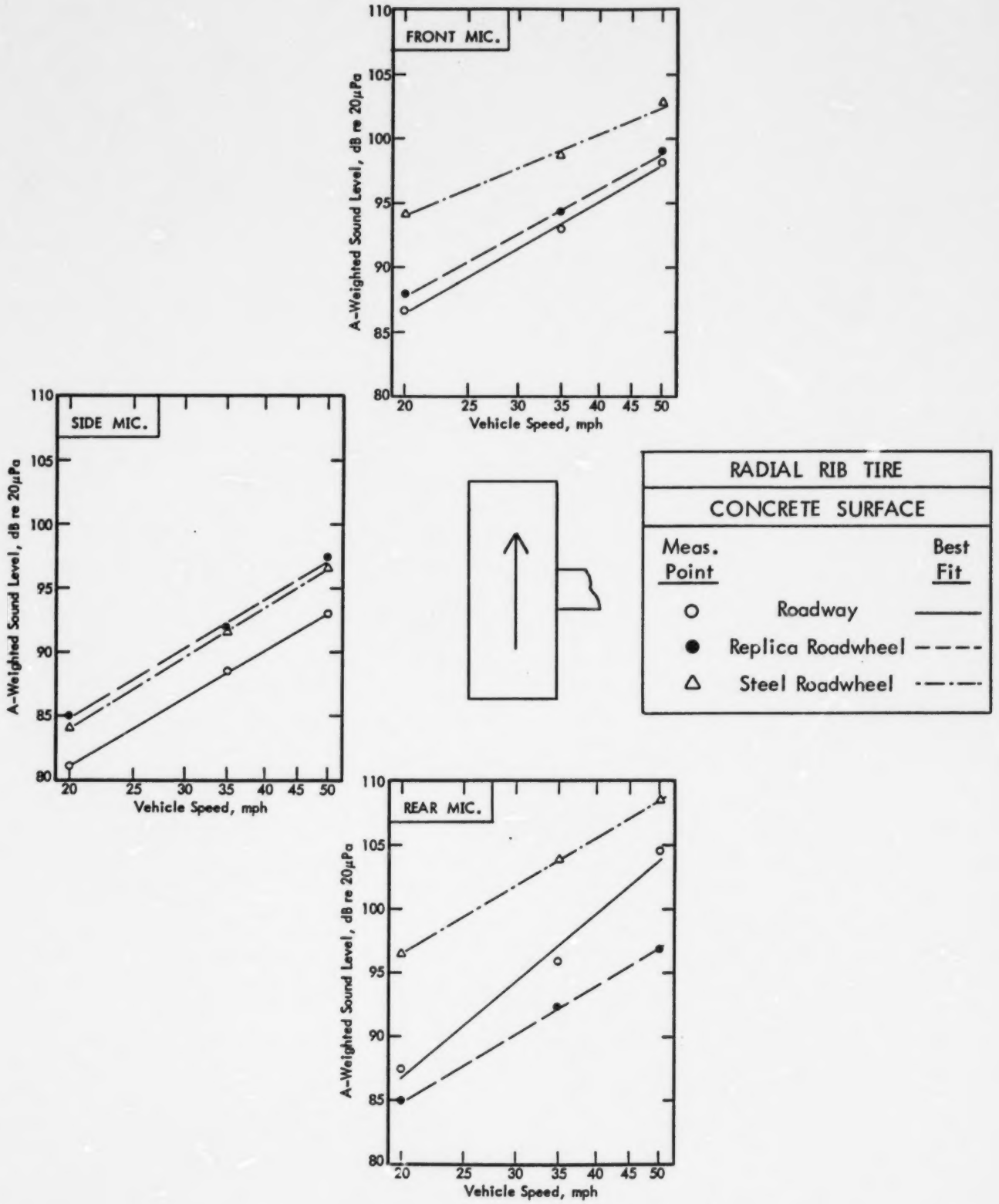

Figure 35 (a). A-Weighted Sound Level Versus Vehicle Speed as a Function of Surface Type for Radial Rib Tire and Concrete Surfaces.

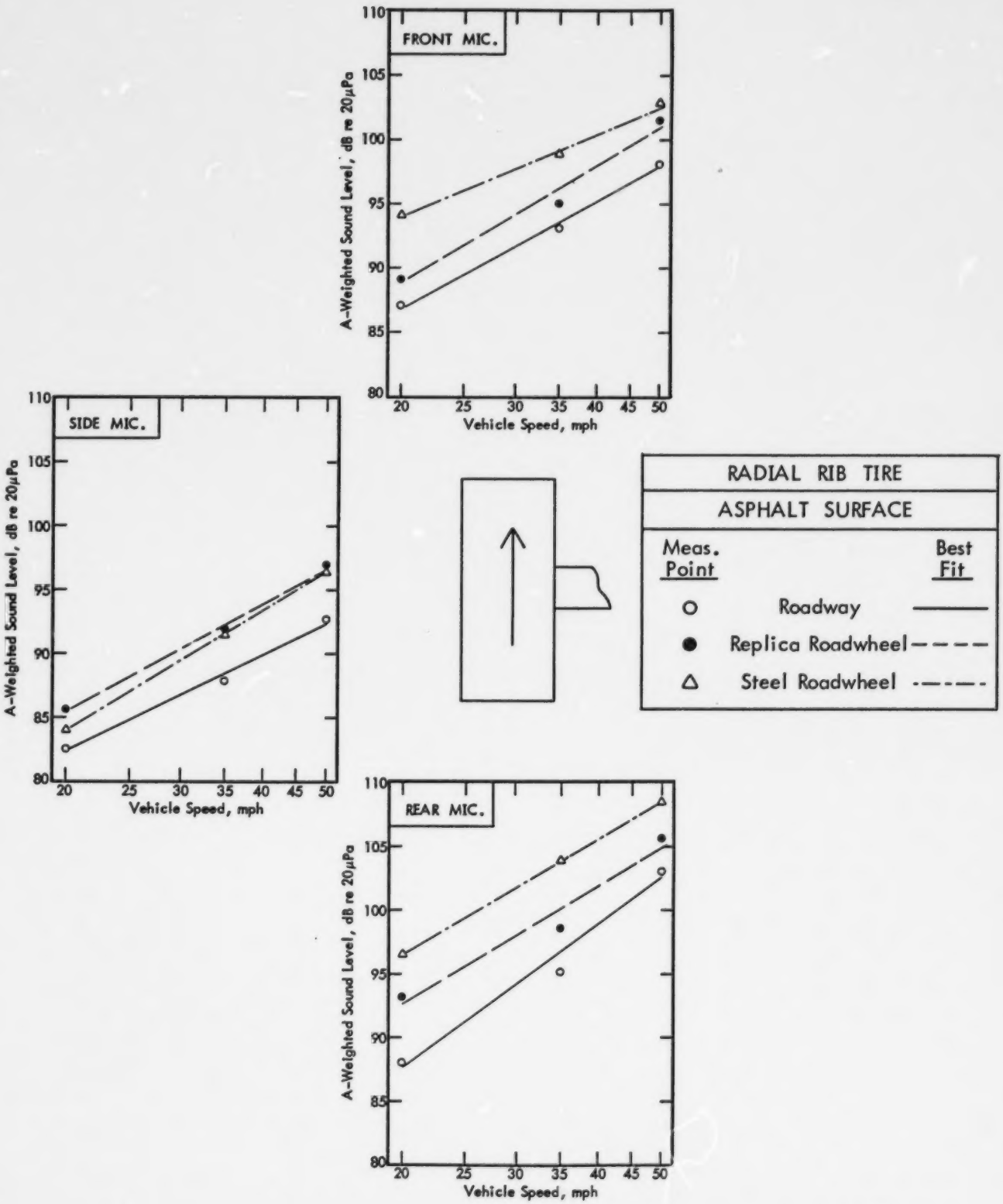

Figure 35 (b). A-Weighted Sound Level Versus Vehicle Speed as a Function of Surface Type for Radial Rib Tire and Asphalt Surfaces.

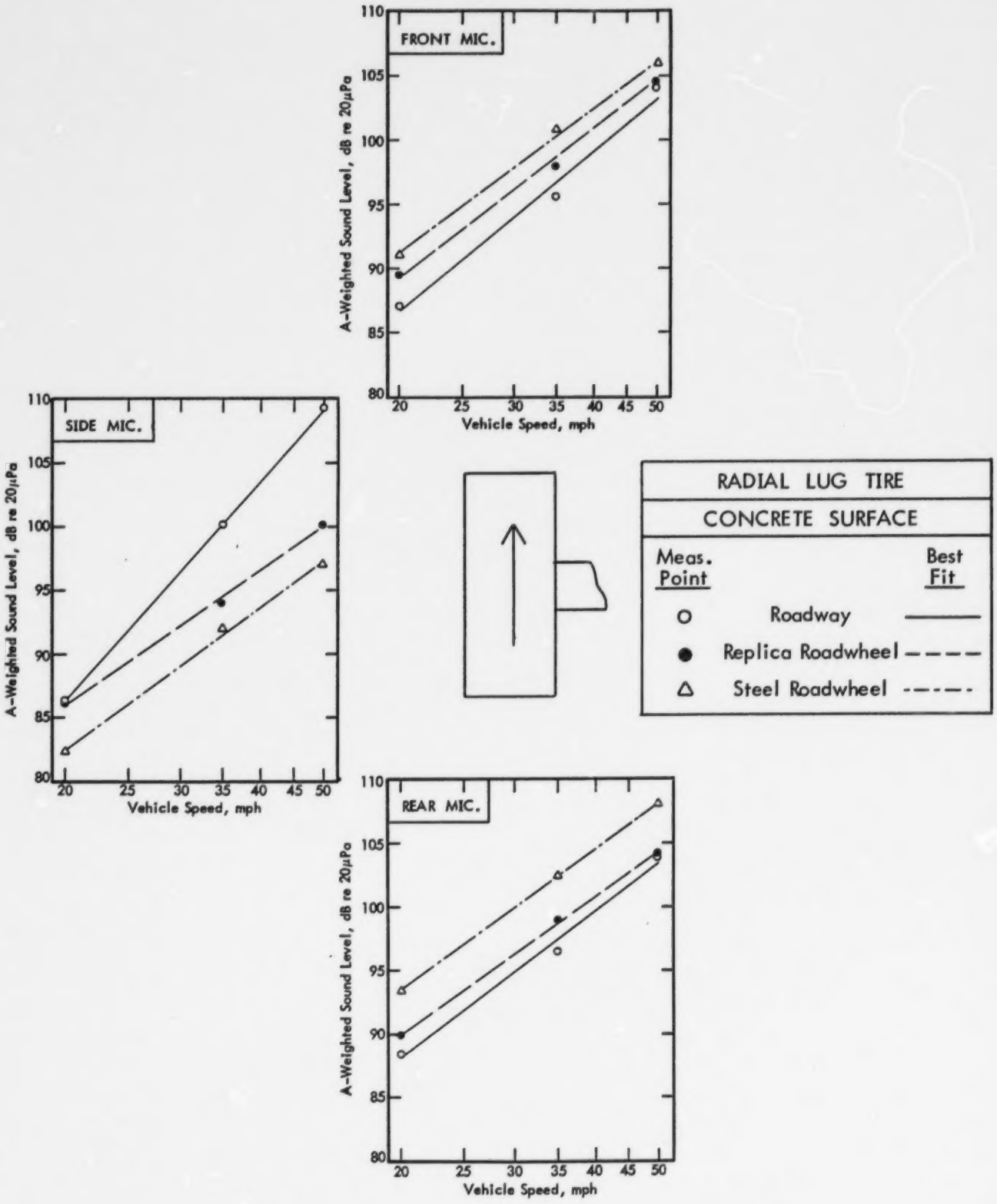

Figure 36 (a). A-Weighted Sound Level Versus Vehicle Speed as a Function of Surface Type for Radial Lug Tire and Concrete Surfaces.

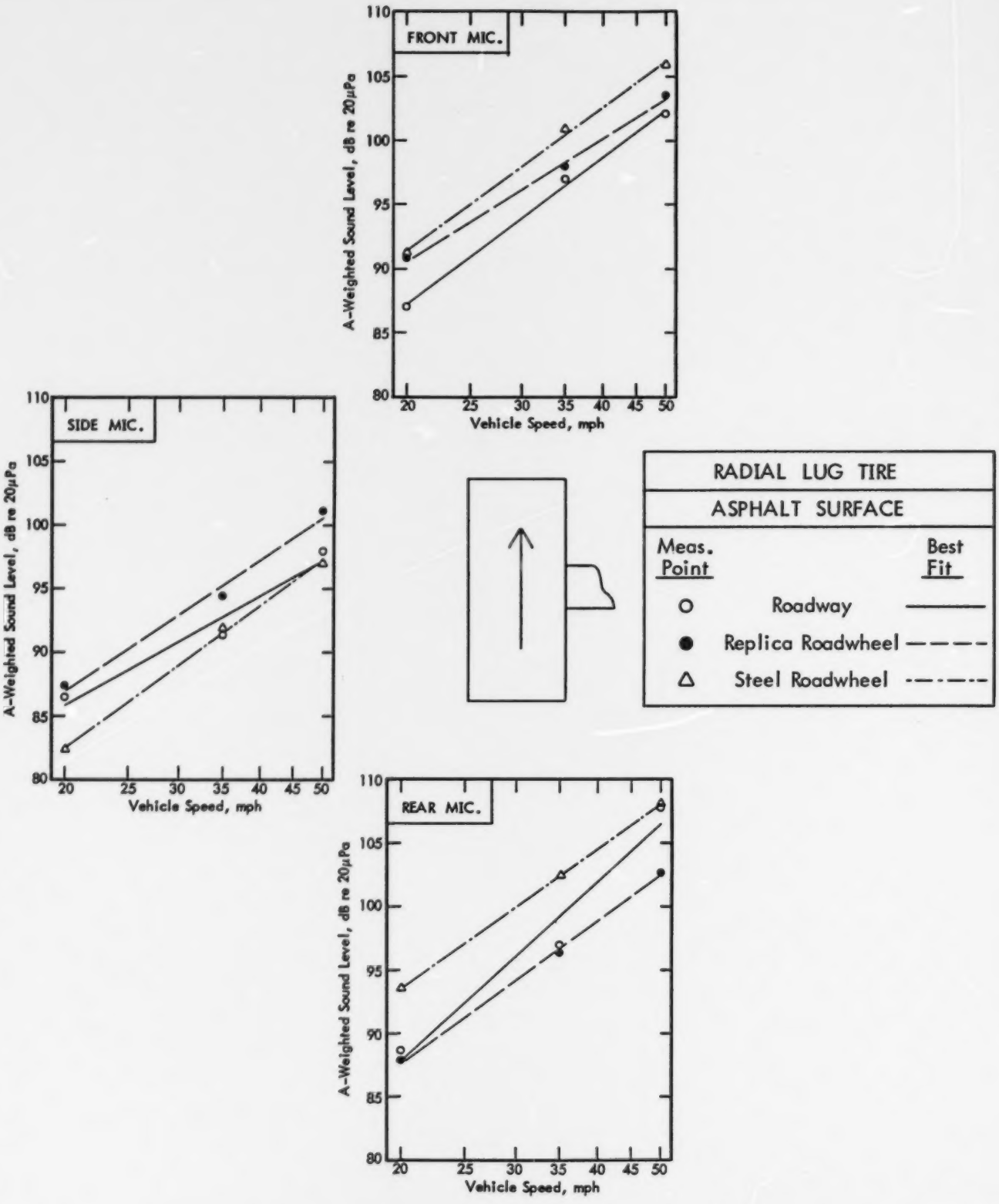

Figure 36 (b). A-Weighted Sound Level Versus Vehicle Speed as a Function of Surface Type for Radial Lug Tire and Asphalt Surfaces.

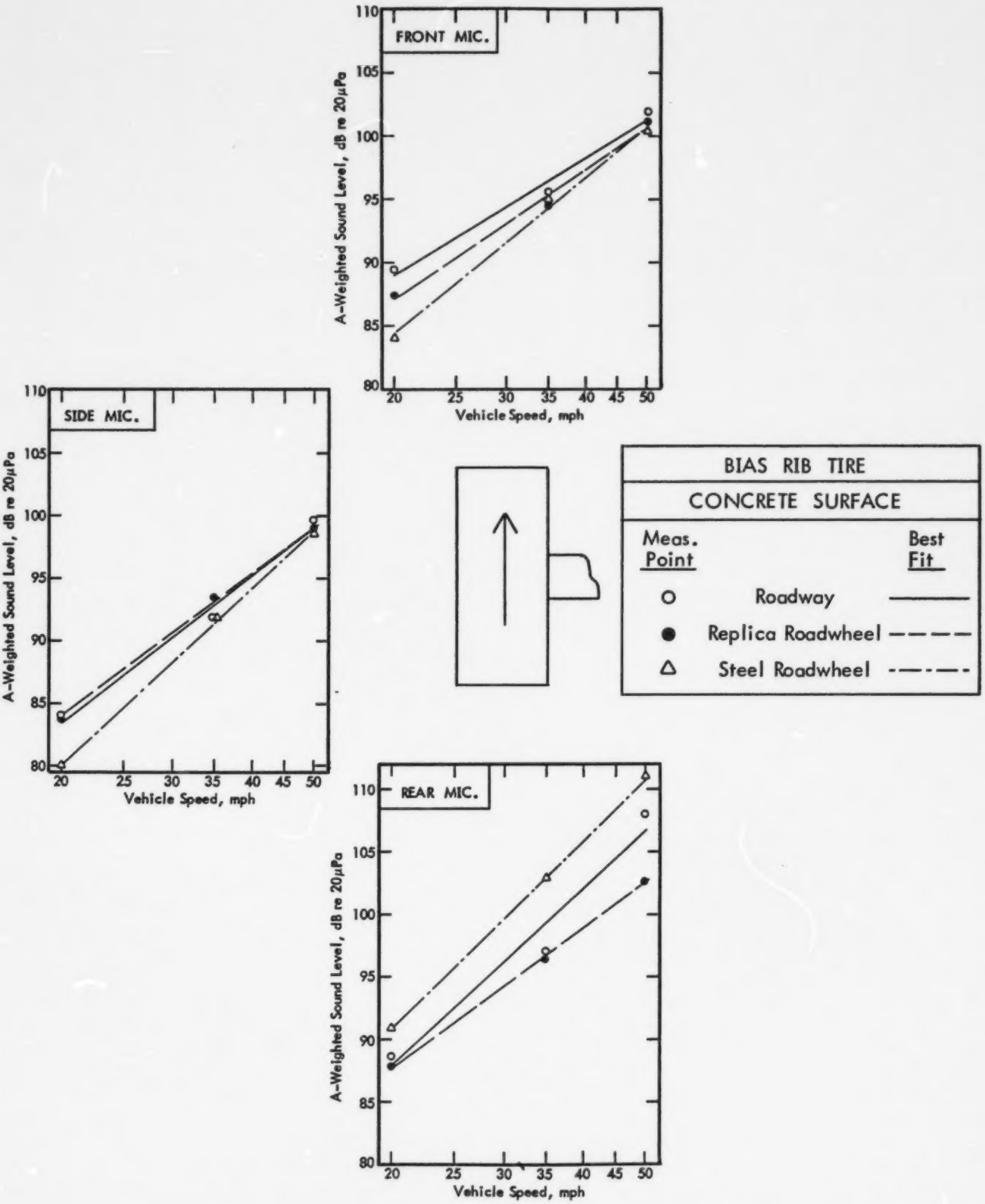

Figure 37 (a). A-Weighted Sound Level Versus Vehicle Speed as a Function of Surface Type for Bias Rib Tire and Concrete Surfaces.

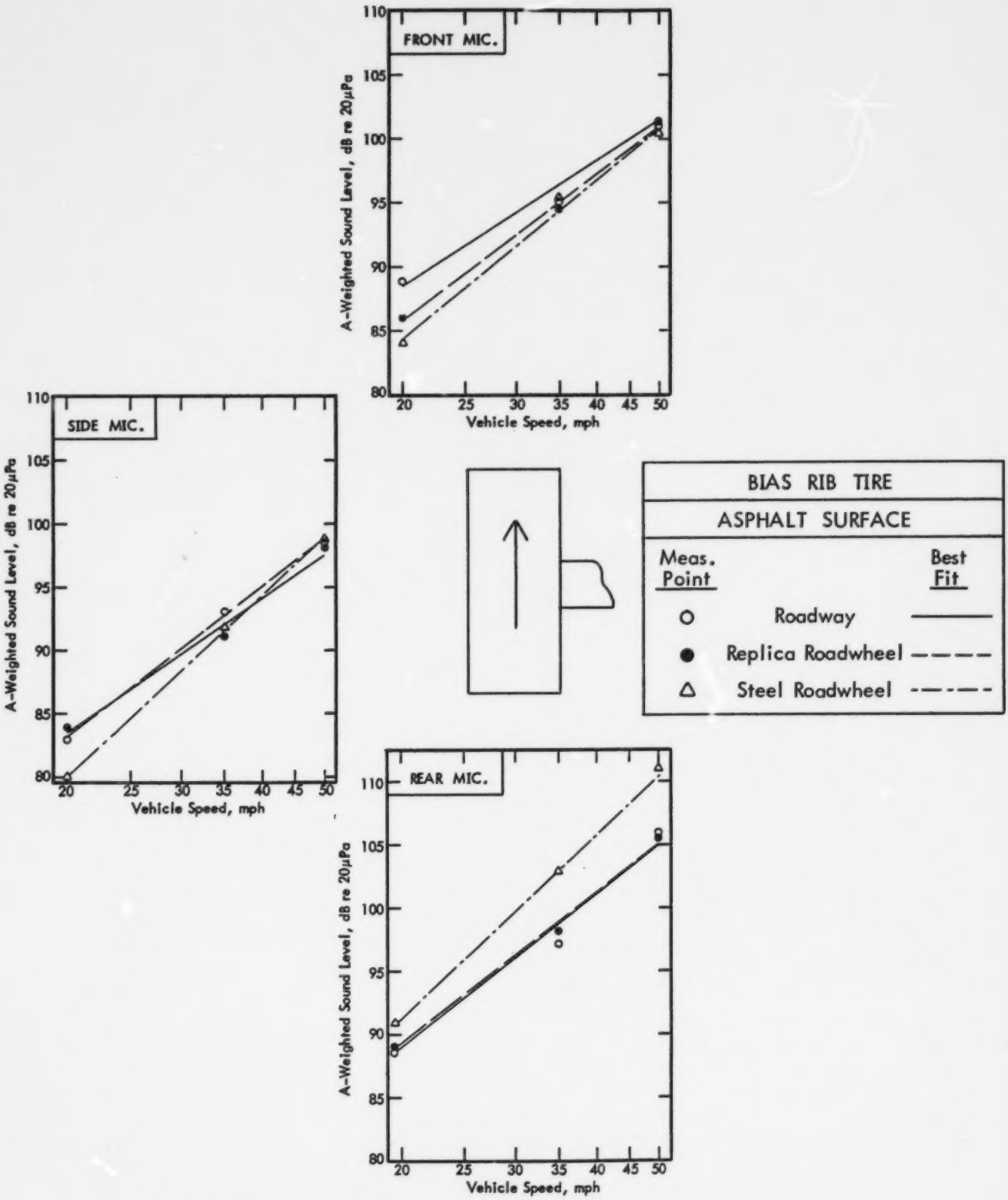

Figure 37 (b). A-Weighted Sound Level Versus Vehicle Speed as a Function of Surface Type for Bias Rib Tire and Asphalt Surfaces.

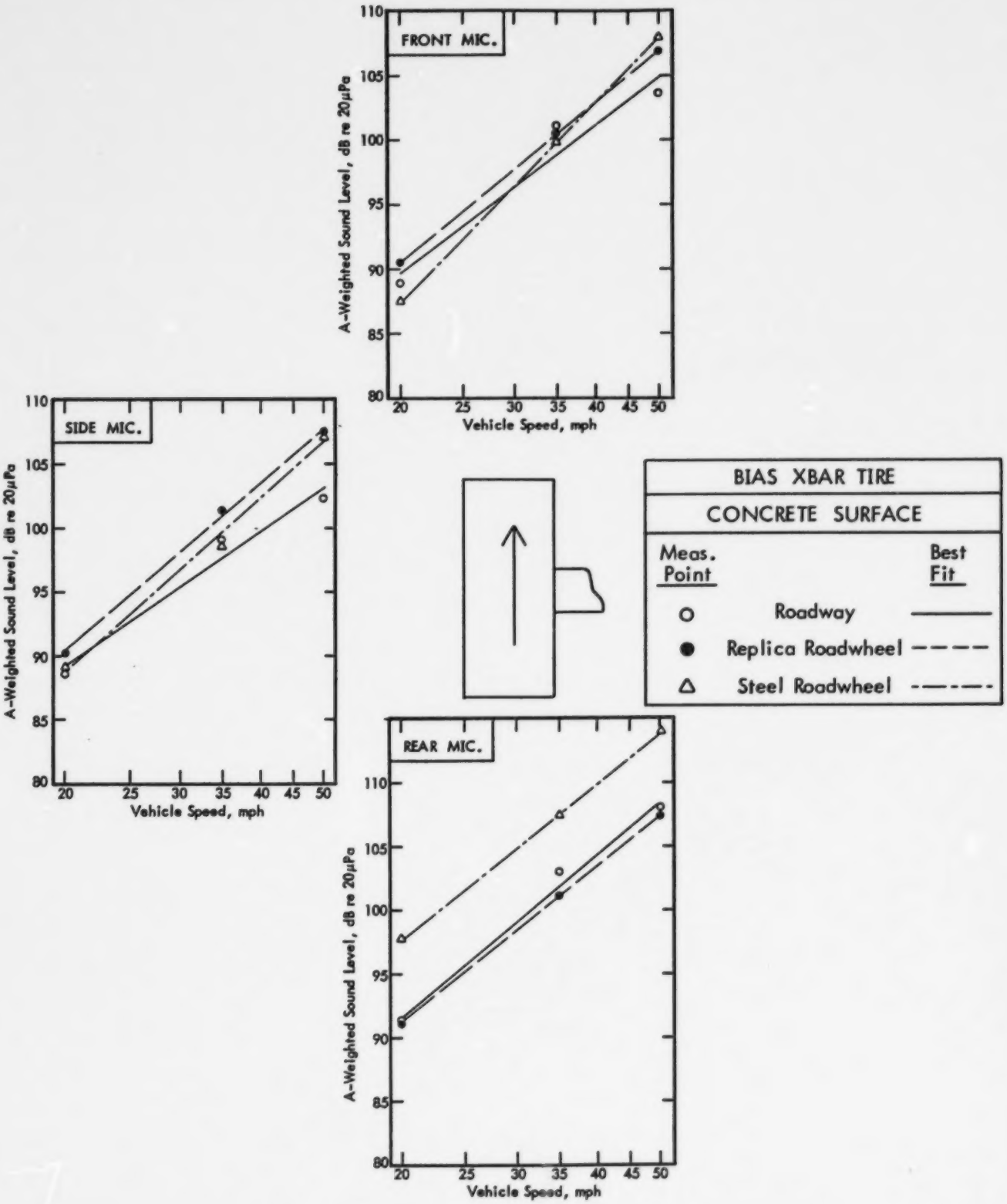

Figure 38 (a). A-Weighted Sound Level Versus Vehicle Speed as a Function of Surface Type for Bias Crossbar Tire and Concrete Surfaces.

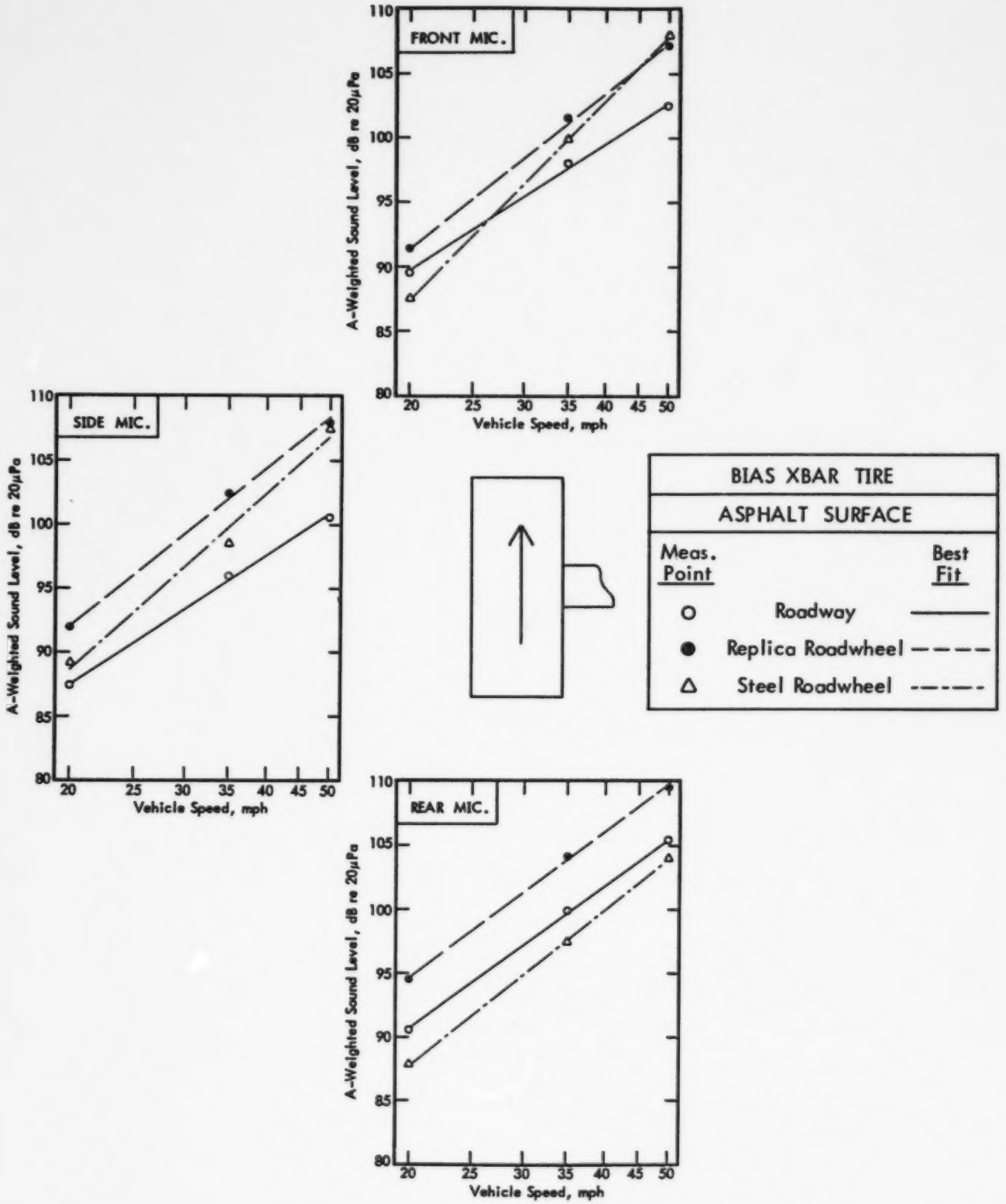

Figure 38 (b). A-Weighted Sound Level Versus Vehicle Speed as a Function of Surface Type for Bias Crossbar Tire and Asphalt Surfaces.

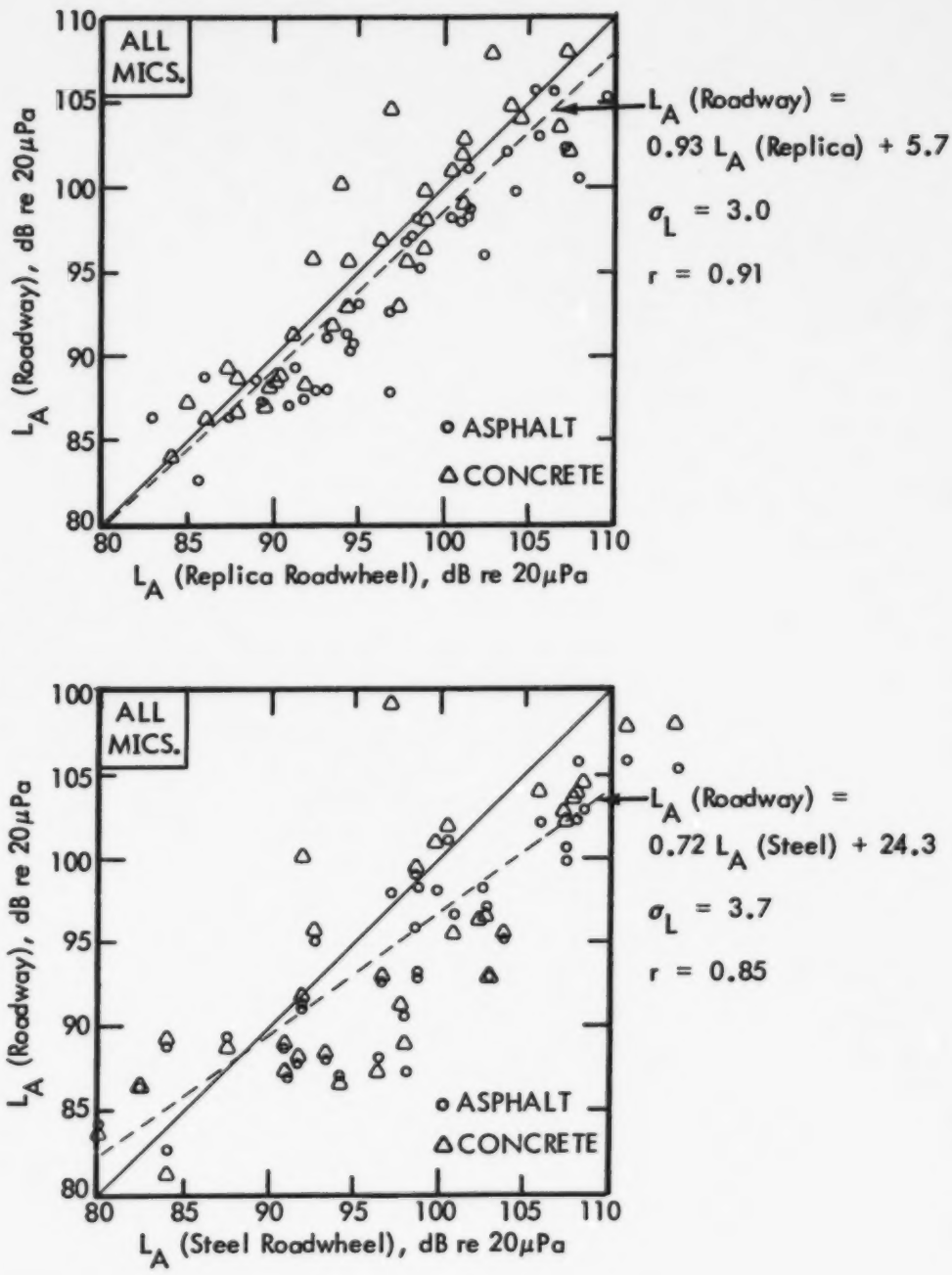

Figure 39. Best Linear Fit of Roadway Levels to Roadwheel Levels for All Tires, Both Roadway Surfaces, All Vehicle Speeds, and All Microphone Positions.

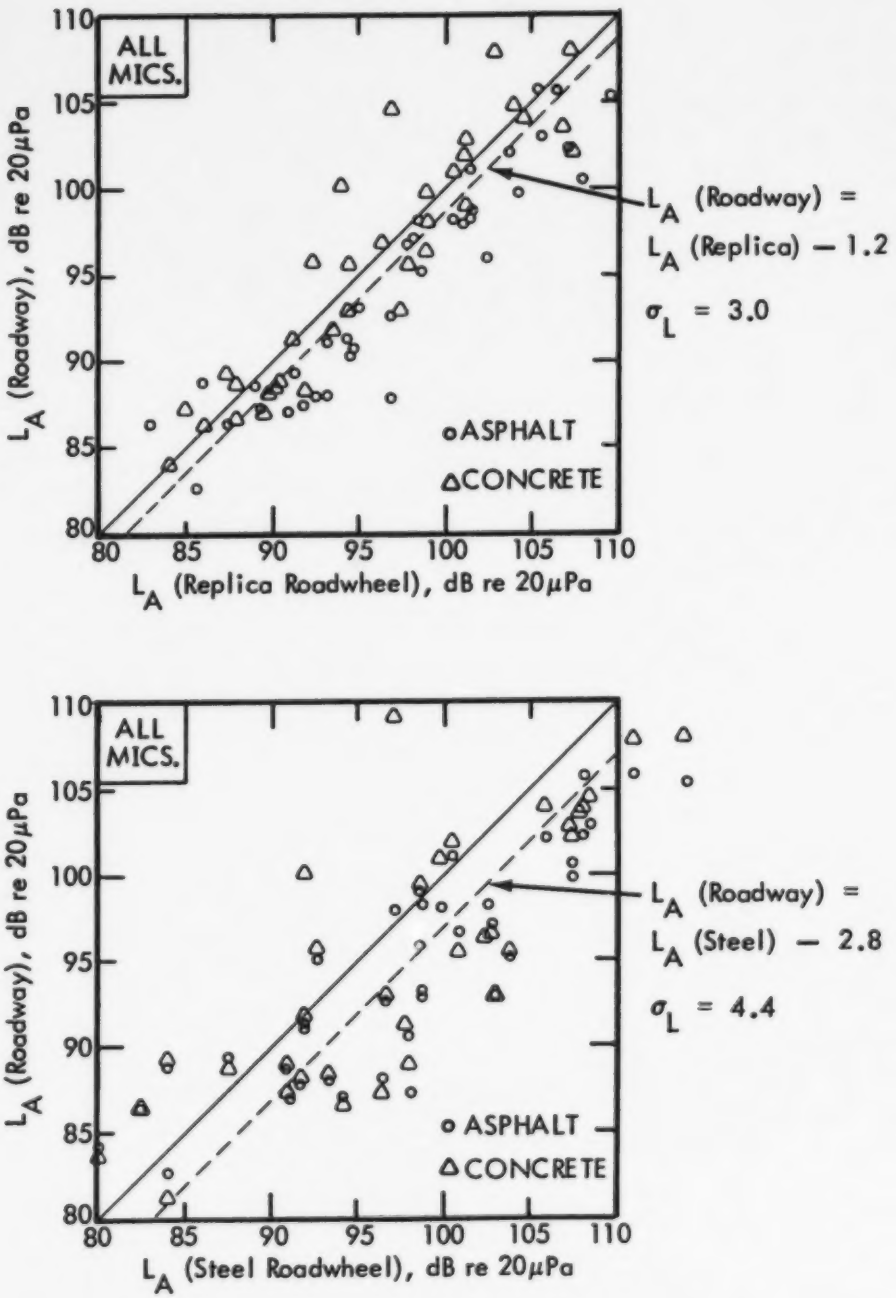

Figure 40. Best Unit-Slope Linear Fit of Roadway Levels to Roadwheel Levels for All Tires, Both Roadway Surfaces, All Vehicle Speeds, and All Microphone Positions.

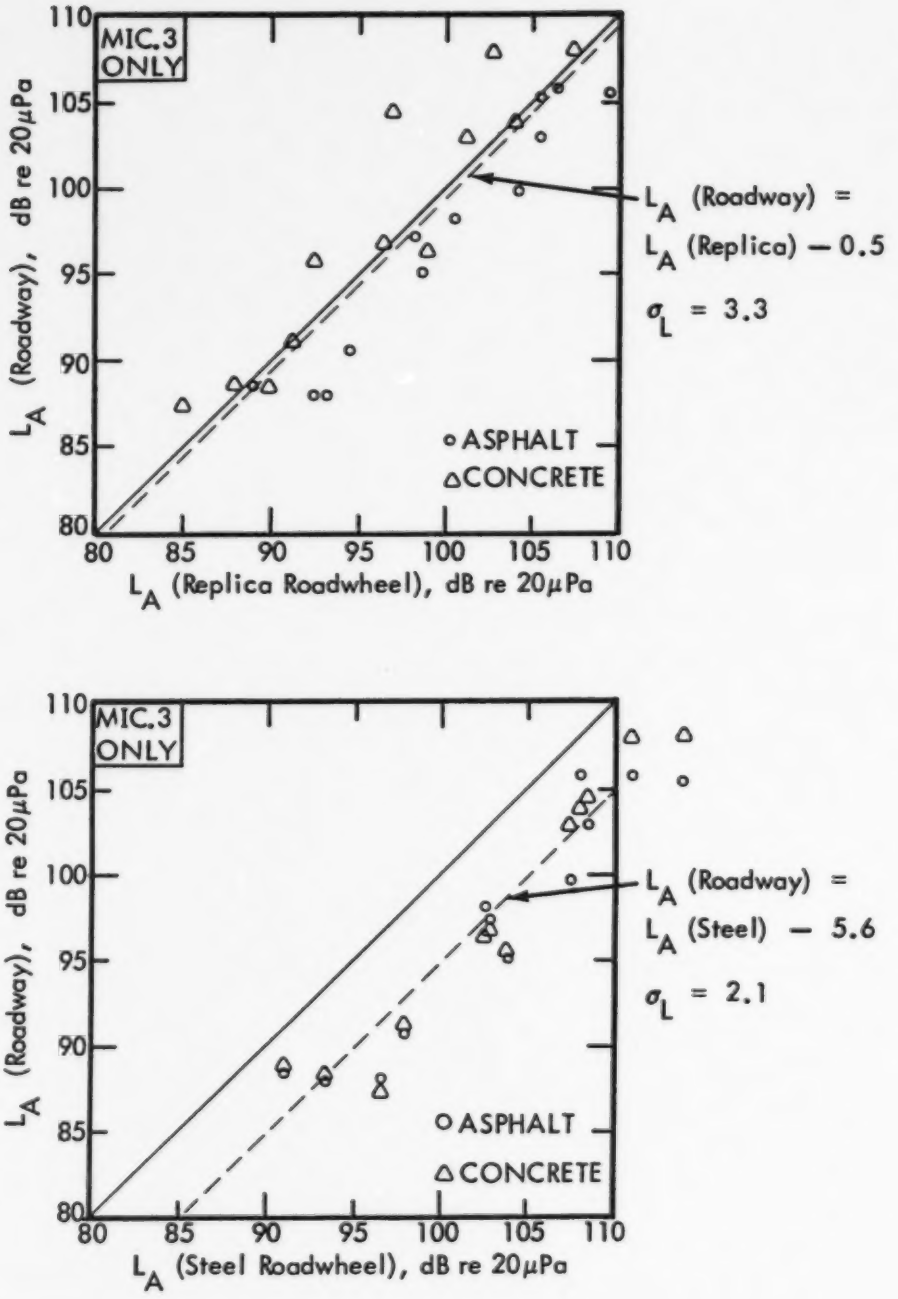

Figure 41. Best Unit-Slope Linear Fit of Roadway Levels to Roadwheel Levels for All Tires, Both Roadway Surfaces, All Vehicle Speeds, and Microphone 3 Only.

4.1.4 Comparison of Steel Plate and Steel Roadwheel Results

In the comparison of roadway and replica roadwheel data in the previous section, two parameters are allowed to vary – the material of which each surface is composed and the curvature of each surface. In order to investigate the effects of curvature only, coastby sound levels on a flat steel plate were compared with levels obtained in a previous program[2] on a curved steel roadwheel. Although the flat steel plate was relatively smooth (see Figure 25), no attempt was made to polish it to the degree of smoothness present on the roadwheel.

Figures 42 through 45 show the measured A-weighted sound levels at each microphone position as a function of vehicle speed and surface curvature (i.e., flat steel plate and steel roadwheel) for each of the four tires tested. Note that because of the difficulty of properly traversing the narrow plate at high speed, there is no 50 mph data for the steel plate.

This data is summarized in Figure 46 which shows the best-fit linear relationship between the flat steel plate levels and the steel roadwheel levels. Figure 47 shows a similar plot in which the best unit-slope linear relationship is shown. In both cases the scatter of data about the best-fit line is sufficiently large that it is not possible to state with certainty that the two sets of levels are different. This would imply that the effect of curvature alone on the sound levels is minimal. This conclusion is in full agreement with the recent study by Donavan and Oswald,[13] where a set of tires were tested on a variety of surfaces and roadwheel diameters.

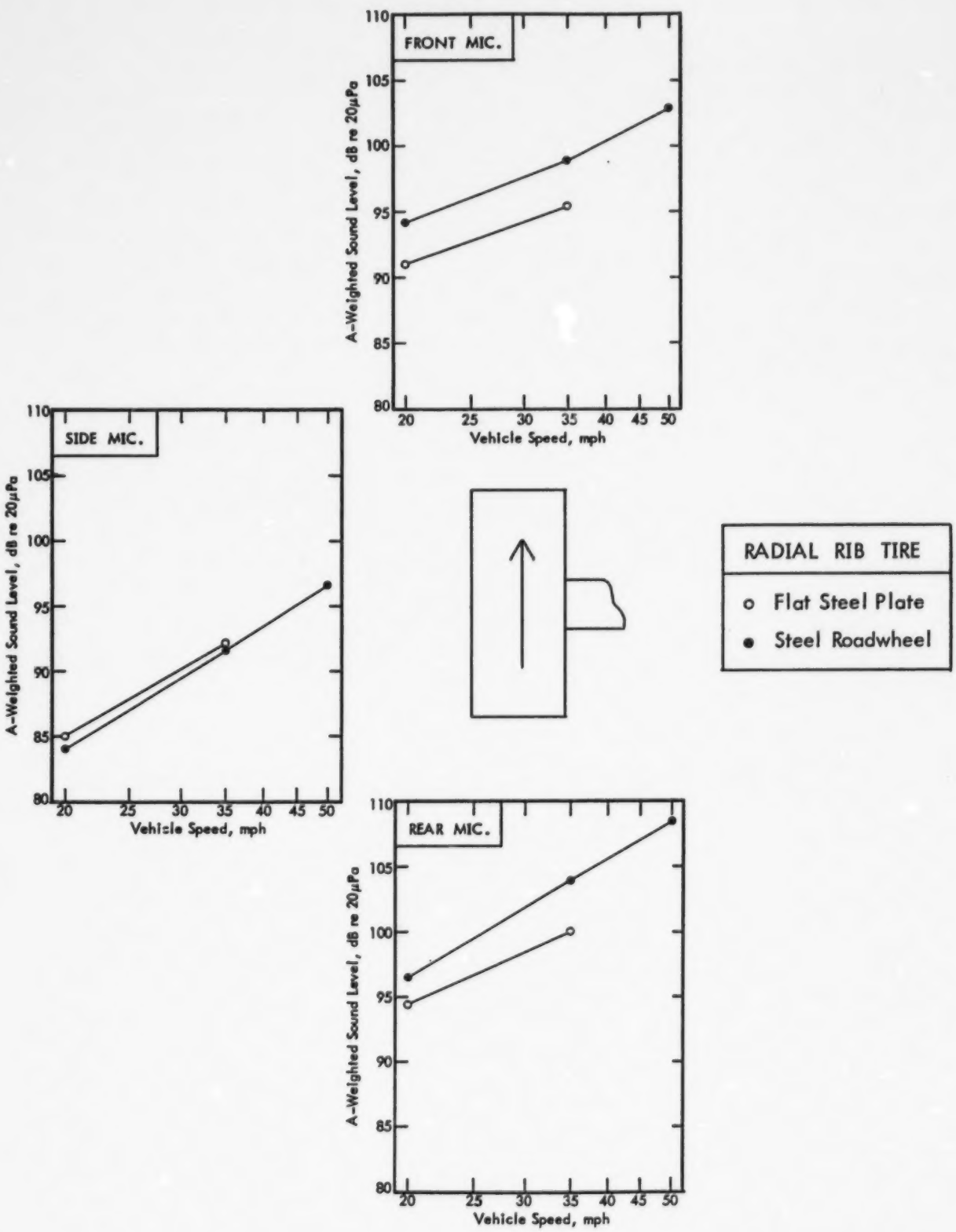

Figure 42. A-Weighted Sound Level Versus Vehicle Speed as a Function of Surface Curvature for Radial Rib Tire.

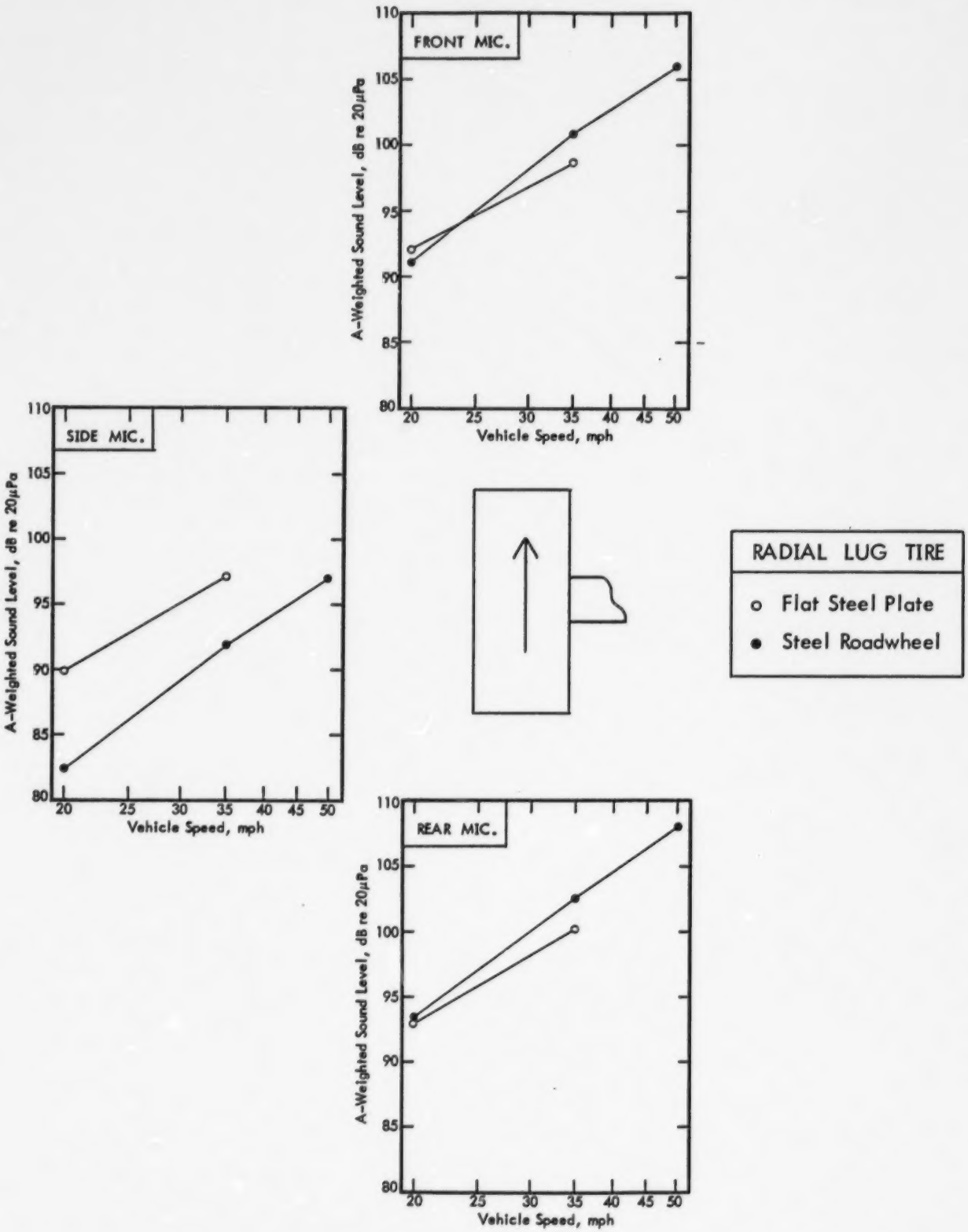

Figure 43. A-Weighted Sound Level Versus Vehicle Speed as a Function of Surface Curvature for Radial Lug Tire.

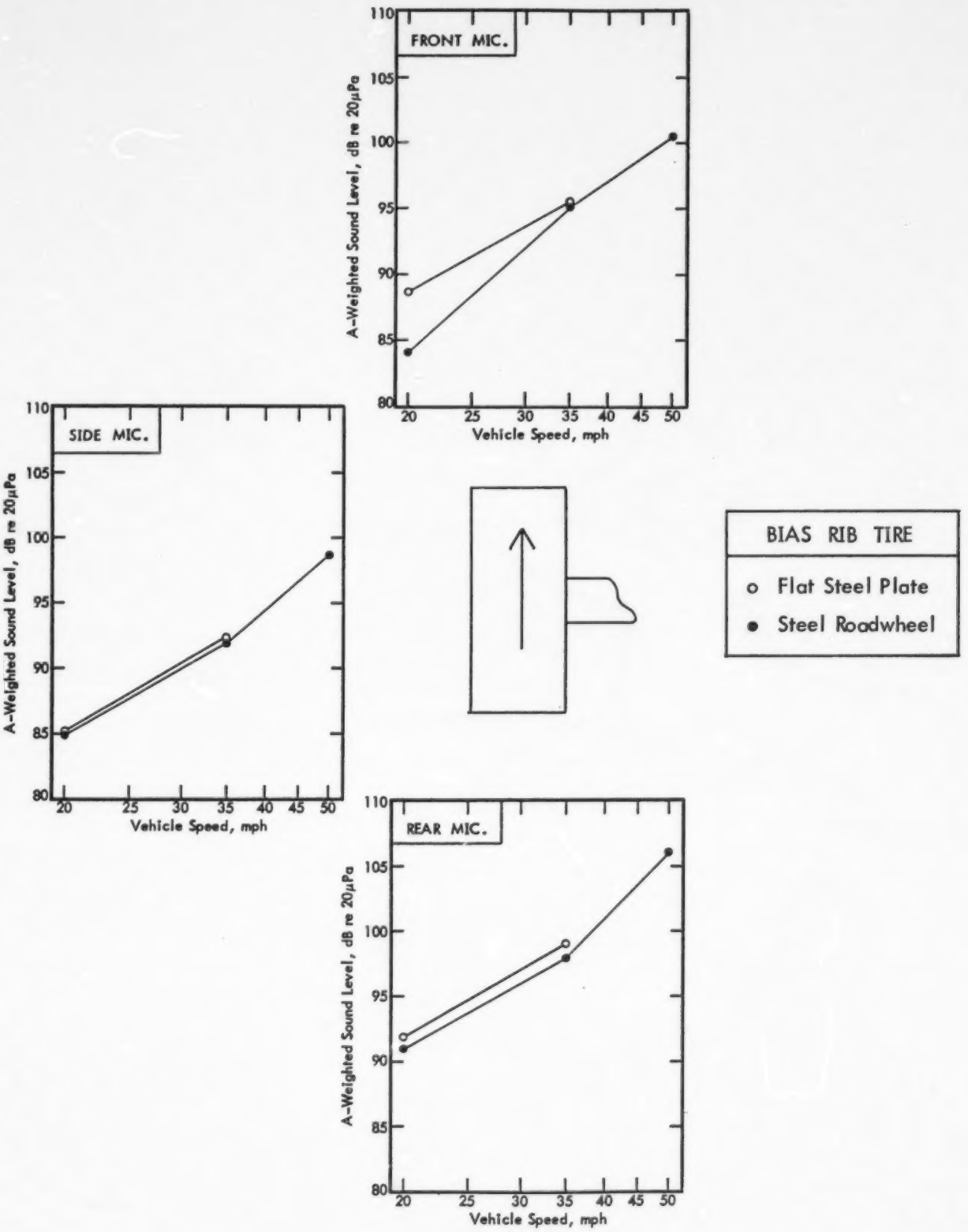

Figure 44. A-Weighted Sound Level Versus Vehicle Speed as a Function of Surface Curvature for Bias Rib Tire.

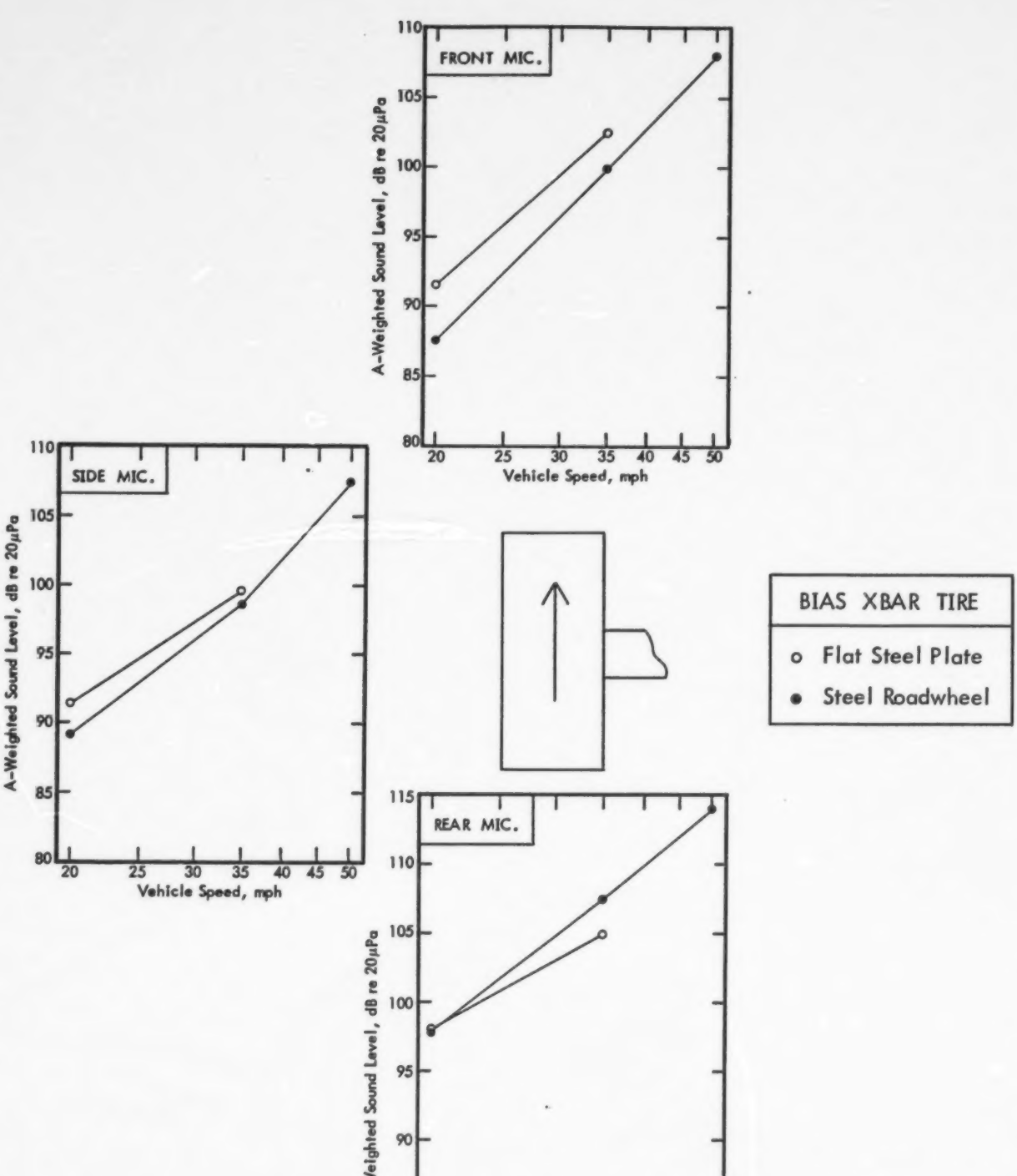

Figure 45. A-Weighted Sound Level Versus Vehicle Speed as a Function of Surface Curvature for Bias Crossbar Tire.

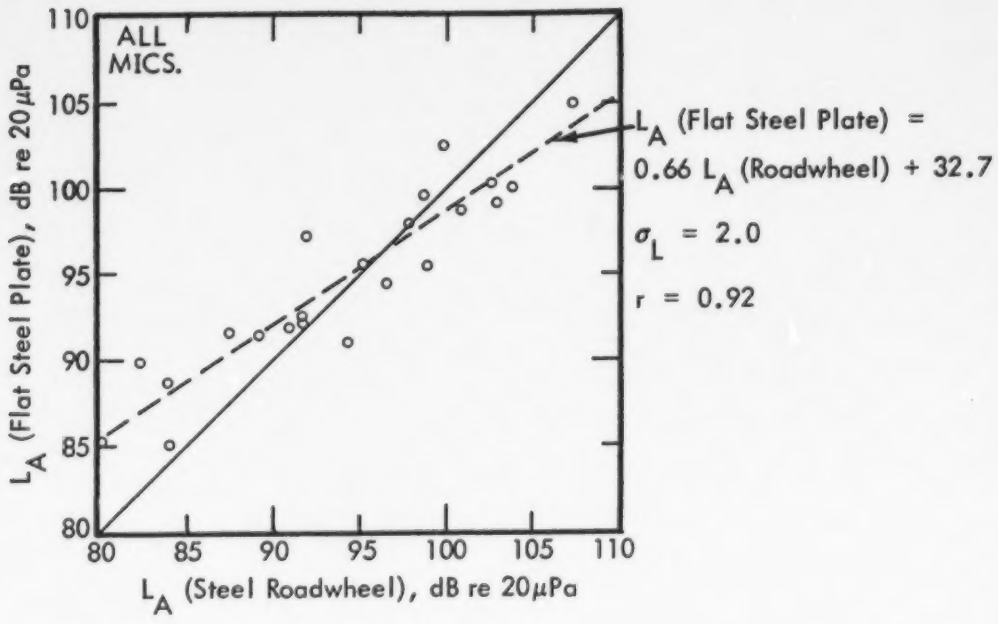

Figure 46. Best Linear Fit of Flat Steel Plate Levels to Steel Roadwheel Levels for All Tires, All Microphone Positions, and Two Vehicle Speeds.

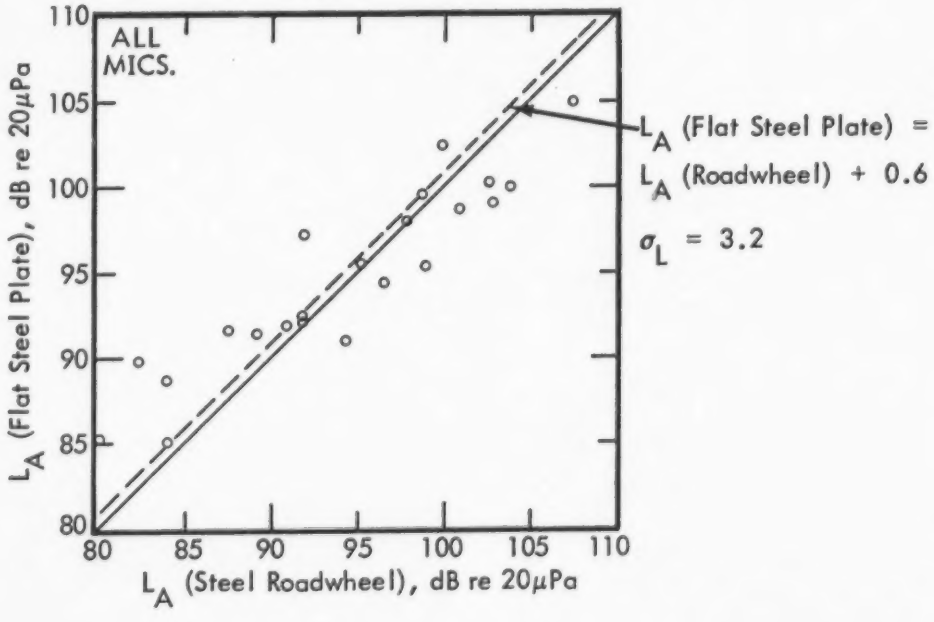

Figure 47. Best Unit-Slope Linear Fit of Flat Steel Plate Levels to Steel Roadwheel Levels for All Tires, All Microphone Positions, and Two Vehicle Speeds.

4.2 Spectra and Time Signatures

4.2.1 Spectra

The analysis of the previous section showed that A-weighted sound pressure levels measured on real and replica surfaces are in good agreement, and that this agreement is better than that between real surfaces and a plain steel roadwheel. To justify the use of the replica, it is necessary that spectral shapes agree as well. Accordingly, spectra were compared for the same data set as discussed in Section 4.1.3. Figure 48 shows a representative set of spectra for one test point. These spectra are not entirely typical, but were selected because they clearly exhibit certain general trends seen in most of the data. These trends are:

- There is no dramatic difference between spectral shapes.
- The replica tends to agree better with the real surface than does the steel. The analysis of A-weighted levels provides a quantitative measure of agreement in the middle frequency range. The agreement of the replica at high frequencies was generally better than the steel, although no consistent high versus low trend was observed.
- At low frequencies, spectral levels on steel tend to be low while those on the replica surfaces tend to be high. The low levels on steel are reasonable since this occurs at frequencies lower than the tread element passage frequency, and the steel drum has no large-scale roughness. The higher levels on the replica may be due to corrugations in the replica shells or due to the small size of the test chamber. The first room mode is around 100 Hz, and the thickness of the absorptive material corresponds to a quarter wavelength at 500 Hz; the performance of the room is therefore less than ideal at frequencies below a few hundred Hz.

While a formal statistical analysis of spectra has not been conducted, it appears that the quantitative agreement in A-weighted levels shown in Section 4.1.3 represents an overall trend. The conclusion that the replica shells provide a valid simulation may therefore be extended to include spectra in the frequency range shown in Figure 48.

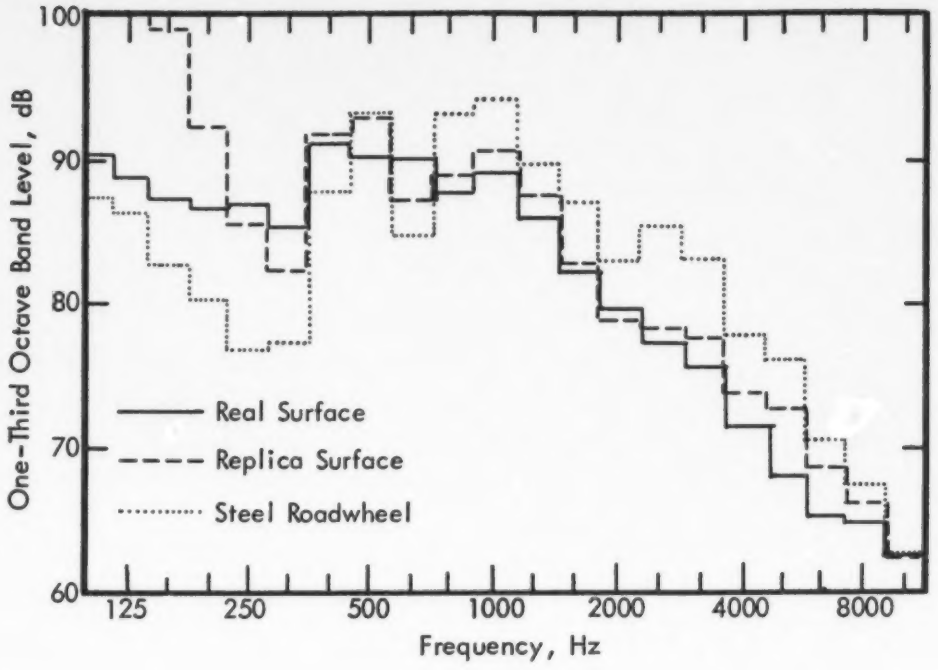

a) Concrete. Radial Lug Tire, Front Microphone.

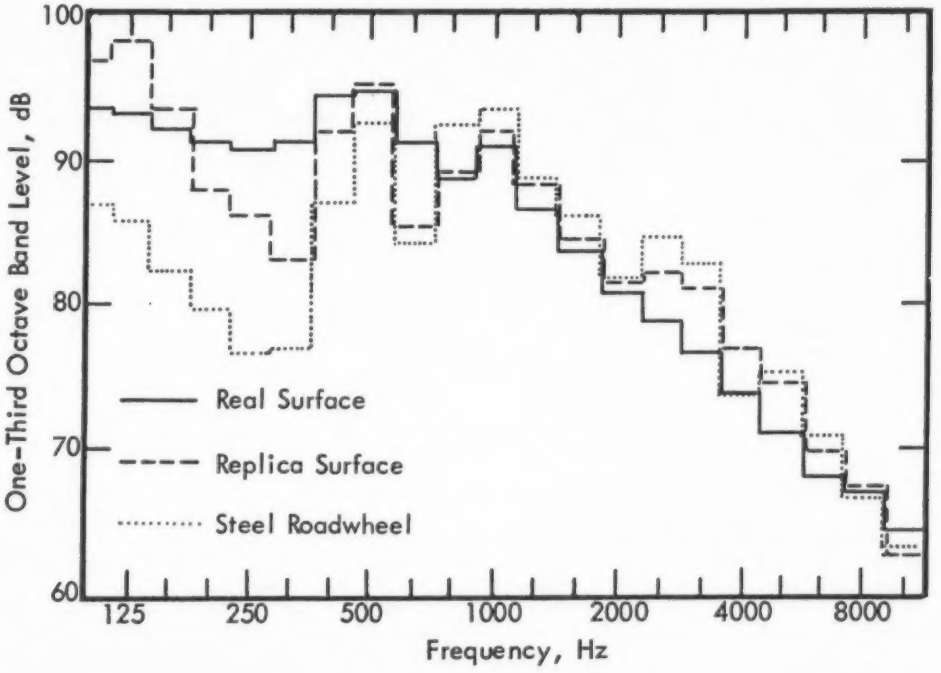

b) Asphalt. Radial Lug Tire, Front Microphone.

Figure 48. Comparison of Spectra on Real, Replica, and Steel Surfaces.

4.2.2 Time Signatures

During measurements on the smooth steel roadwheel, it was observed that time signatures were highly repeatable when captured in synchronization with the tire.[2] Passage of individual elements could be seen quite distinctly. Figure 49 is a typical sound pressure time history, corresponding to the rear of the radial lug tire on the steel roadwheel at 35 mph. Three 8 msec (corresponding to a 5-inch segment of tire passing) samples are shown. These were triggered at the same angular position on three successive revolutions. The samples repeat quite well, with part of the differences seen being due to jitter in the timing pulse. Noise generation is clearly deterministic in this case, and the passage of individual tread elements can be seen. Figure 50 shows similar data for acceleration of the carcass at the center of the tread area. Three 40 msec (corresponding to about 20 inches of the tire) samples are shown. A detailed discussion of the nature of these acceleration data is contained in References 1 and 2. For present purposes, it is sufficient to note that there is a large acceleration impulse associated with the curvature change through the contact patch, plus fine structure associated with carcass vibration-generated noise. The passage through the contact patch is near the center of Figure 50. As with the sound signal, the acceleration data repeat quite well, with fine structure clearly associated with individual tread elements.

This consistency is not seen on a textured surface. Figures 51 through 52 show the same data for one replica surface and the corresponding real surface.* The presence of texture reduces the dependence of noise on the tire alone. This behavior has been previously documented in other studies, wherein signal averaging has been used to isolate "roadwheel" and "tire" components of noise.[10,14] Conditions were observed in this program where time signatures repeated when sampled in synchronization with the roadwheel, with minor variations due to tread. The stochastic element introduced by the replica surface is an important phenomenon which exists on roads. A major effect is that detailed design changes producing changes seen on a smooth drum may not carry through to highways since texture effects can overshadow them. This is a critical factor which makes the simulated texture extremely valuable when performing laboratory evaluation of potential noise-related tire modifications.

---

* All figures are for approximately the same portion of the tire: each sound pressure/acceleration pair is for the same segment, while there are phase differences of several milliseconds between different surfaces.

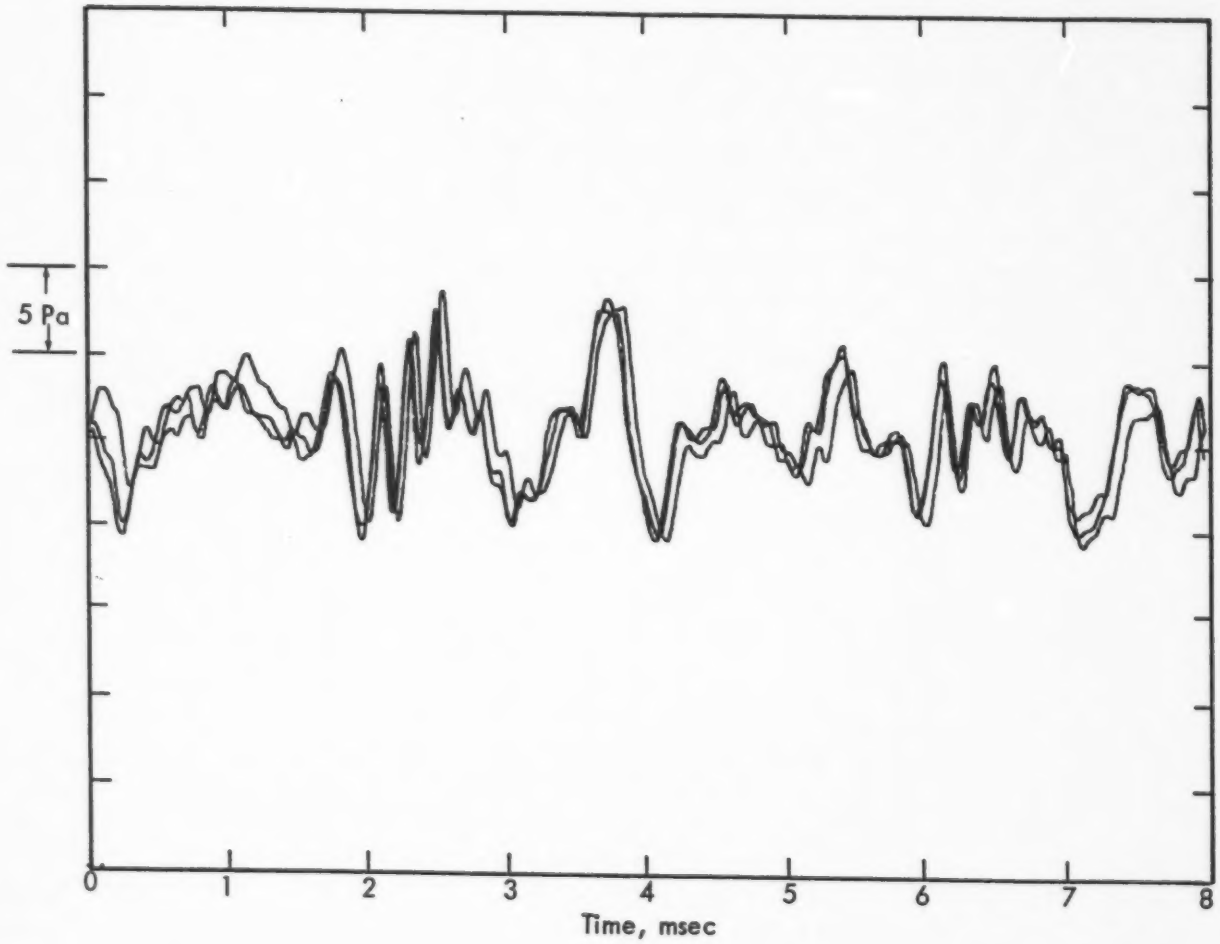

Figure 49. Successive Samples of Sound Pressure on Steel Roadwheel.

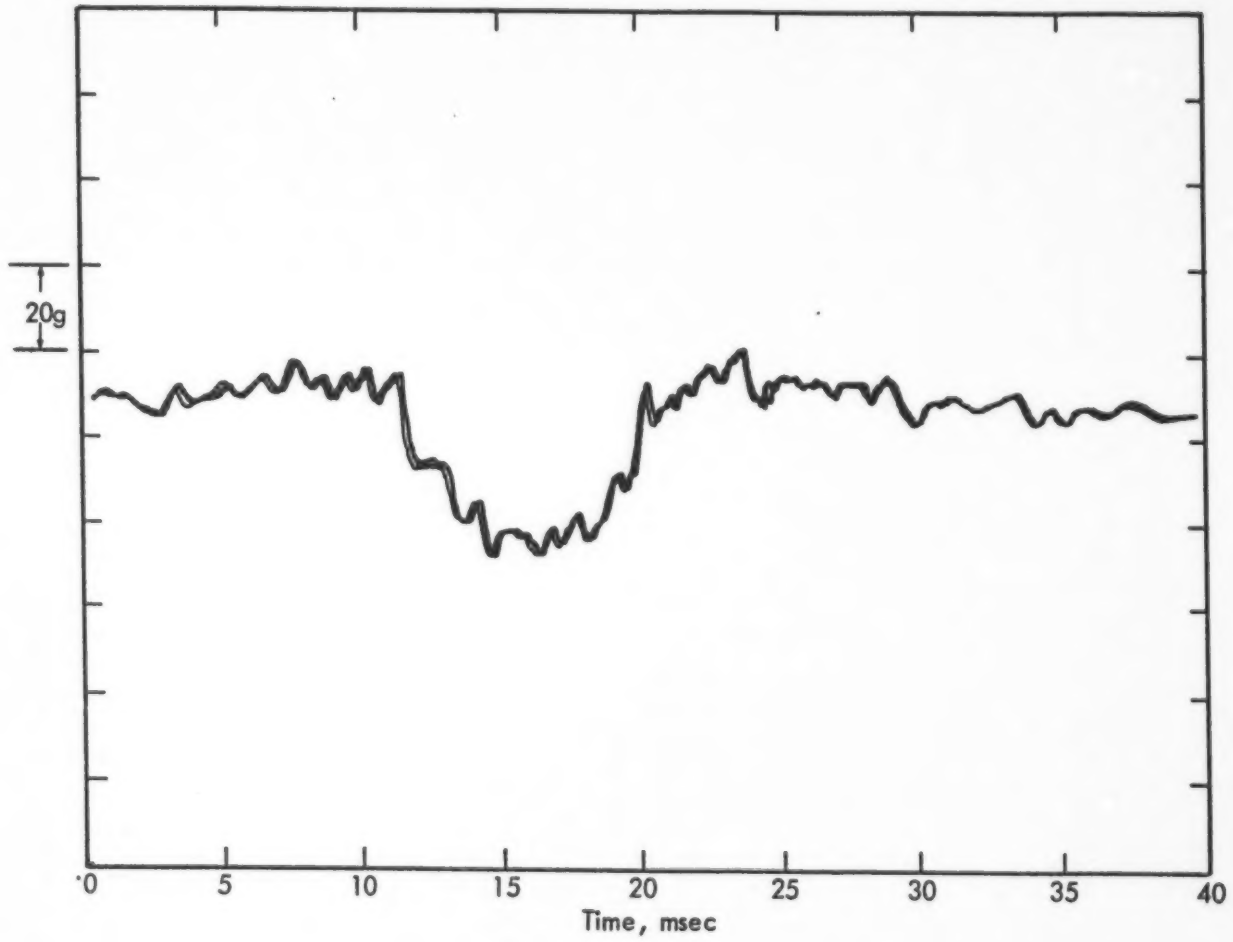

Figure 50. Successive Samples of Carcass Acceleration on Steel Roadwheel.

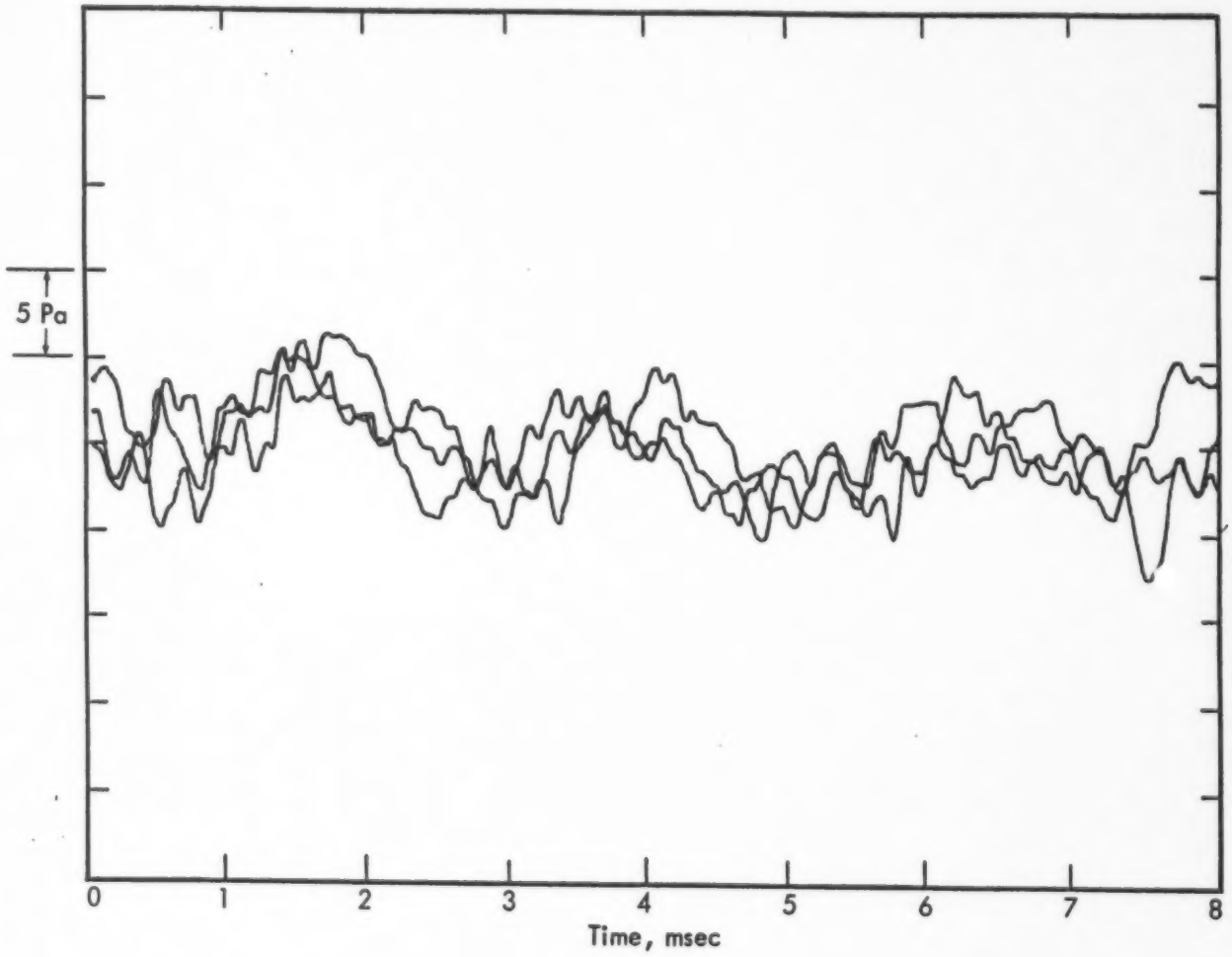

Figure 51. Successive Samples of Sound Pressure on Replica Surface.

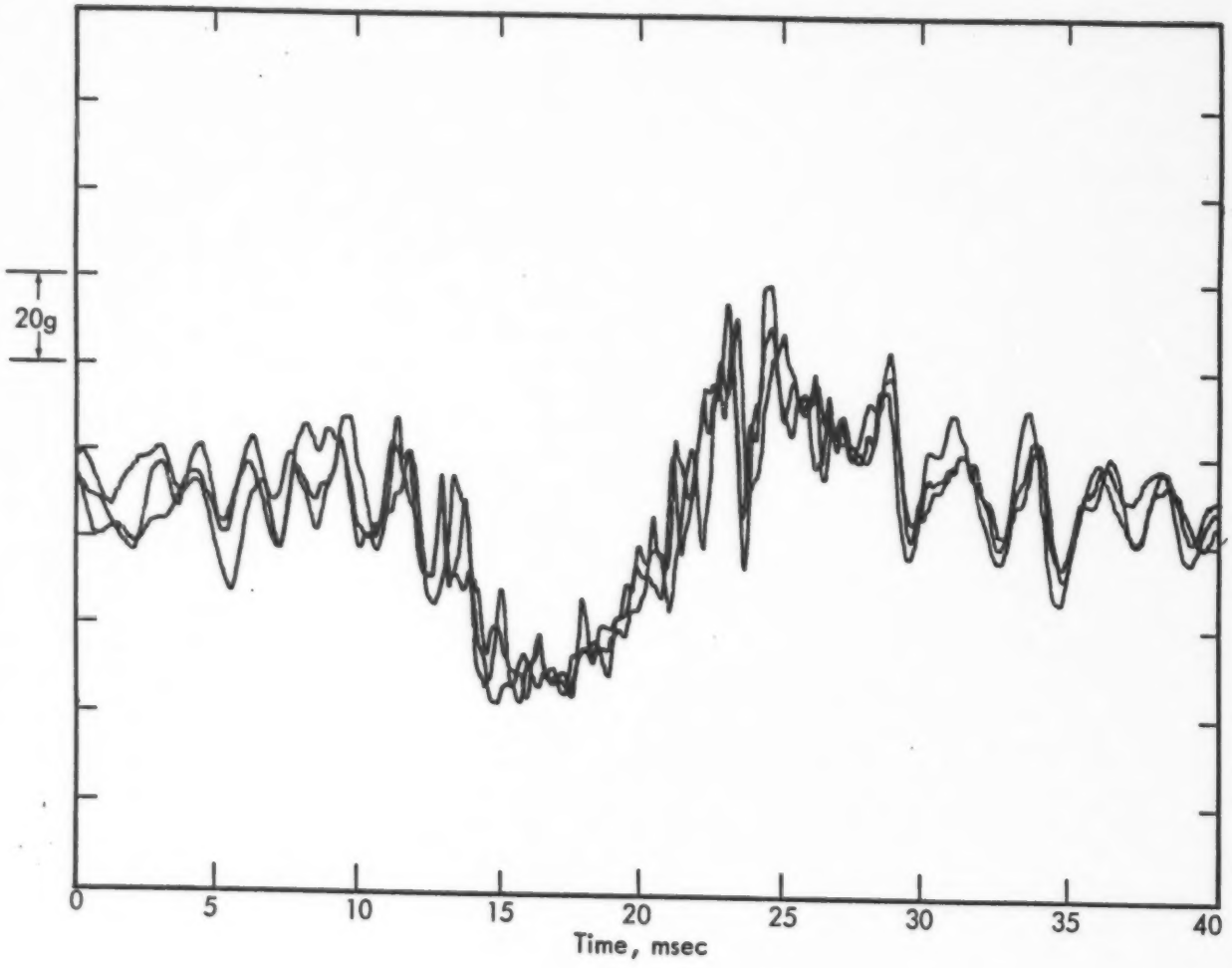

Figure 52. Successive Samples of Carcass Acceleration on Replica Surface.

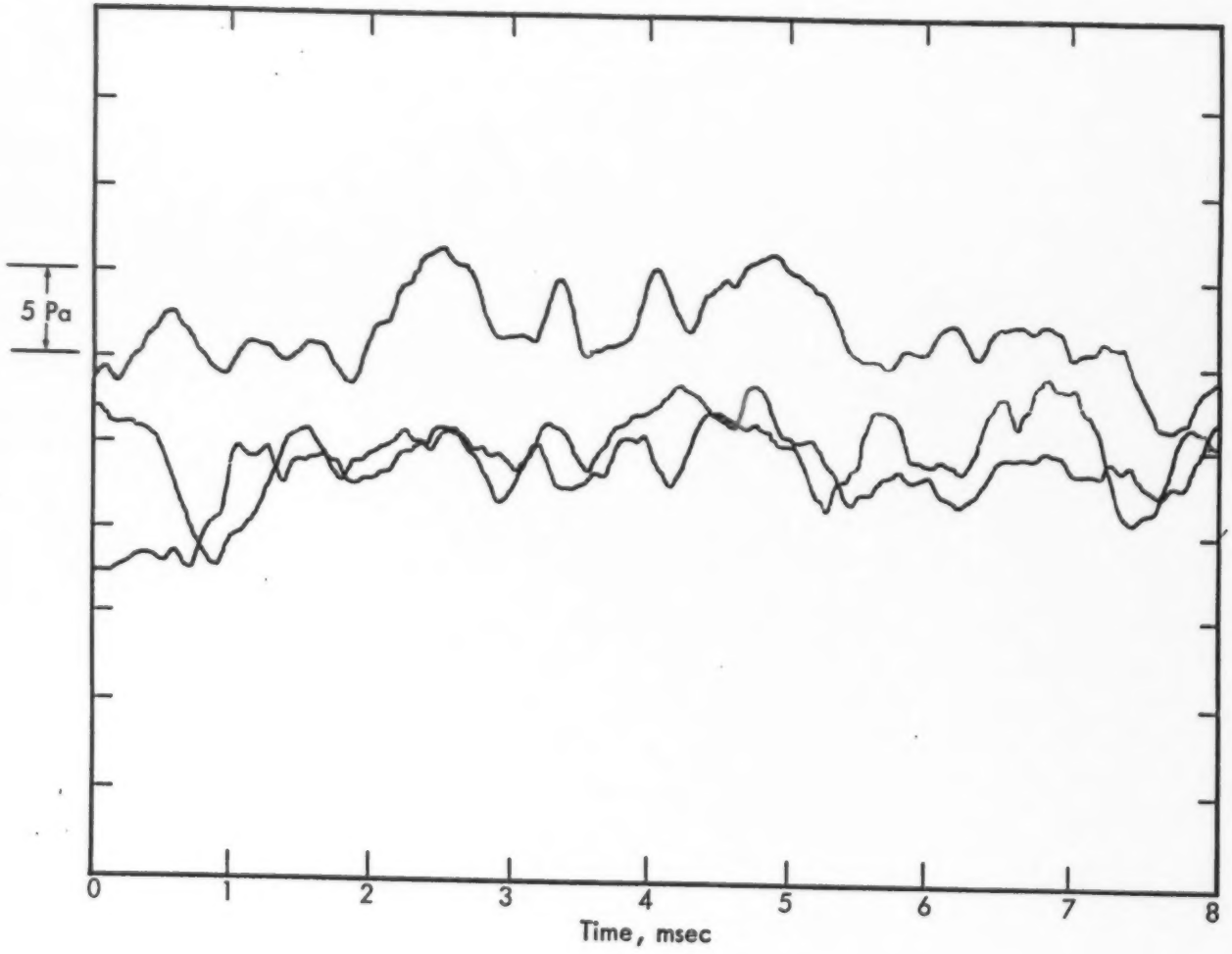

Figure 53. Successive Samples of Sound Pressure on Real Surface.

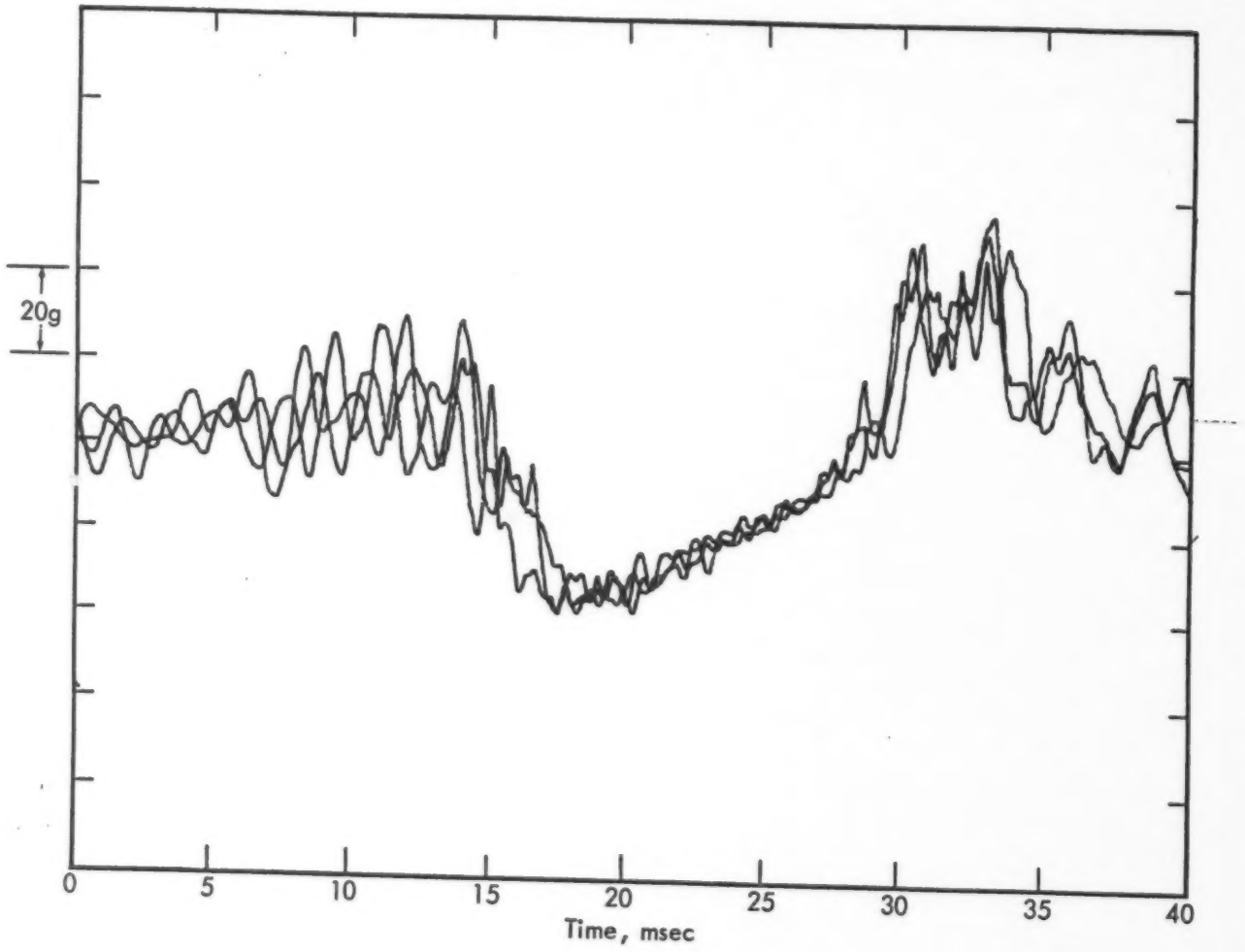

Figure 54. Successive Samples of Carcass Acceleration on Real Surface.

The critical difference noted here is the deterministic/random difference between smooth and textured surfaces. There are also differences between testing on the real and replica surfaces which are worth noting. The repeatability on the replica surface is somewhat better than on the real surface. This is generally to be expected when comparing field versus laboratory data, due to the difference in control available. The field data in general exhibited greater run-to-run variability, including a greater percentage of "bad" data points. This, plus the usual outdoor problems such as weather, were the primary reason for developing the roadwheel facility. The field data also provided non-steady data, since the coasting vehicle was slowly decelerating. The kind of signal averaging described in References 10 and 14 would be very difficult with a coasting vehicle: the sample would be short, and an order sampling arrangement synchronized to the tire would be required.

5.0 CONCLUSIONS

A series of tire near-field noise and carcass vibration measurements have been conducted on real pavement surfaces, flat and curved smooth steel surfaces, and on curved replica pavement surfaces. Four production model heavy truck tires were used for these tests The A-weighted sound levels for the four tires on five real surfaces are presented here, and trends for this data set discussed. A detailed comparison has been made between real surfaces, curved replica surfaces on a roadwheel, and a smooth steel roadwheel. Conclusions of this comparison are:

- The replica surfaces provided a very good simulation of the real surfaces. Both A-weighted levels and spectral shapes showed better agreement between real and replica than between real and smooth steel.
- Comparison between steel roadwheel data and data from a flat steel plate showed good agreement. It is concluded that texture matters more than curvature for noise evaluation.
- Tire noise on a steel surface is deterministic, and exhibits the characteristics of the tire. Tire-road noise on a textured surface has a significant random element, which can be of critical importance in evaluating the practical value of potential noise-related tire modifications.

REFERENCES

1. Plotkin, K.J., and Stusnick, E., "A Unified Set of Models for Tire/Road Noise Generation", Wyle Research Report WR 81-26, July 1981.

2. Plotkin, K.J., Montroll, M.L., and Fuller, W.R., "A Study to Identify Advanced Methods of Reducing Tire Noise", Wyle Research Report WR 80-16, April 1980.

3. Thrasher, D.B., Miller, R.F., and Bauman, R.G., "Effect of Pavement Texture on Tire/Pavement Interaction Noise", SAE Paper 762011, November 1976.

4. Fuller, W.R., "The Influence of Pavement Roughness Upon Tire/Pavement Interaction Noise Levels", paper presented at NOISEXPO, New York, March 1976.

5. Osman, M.M., and May, D.N, "Relative Influence of Pavement Texture and Tire Type on Pavement/Tire Noise", SAE Paper 800282, February 1980.

6. Sandberg, U., "Characterization of Road Surfaces With Respect to Tire Noise", Proceedings of the International Tire Noise Conference, Stockholm, Sweden, August 1979, pp. 227-234.

7. Sandberg, U., and Descornet, G., "Road Surface Influence on Tire Noise – I", Proceedings of InterNoise 80, December 1980, pp. 259-266.

8. Descornet, G., and Sandberg, U., "Road Surface Influence on Tire Noise – II", Proceedings of InterNoise 80, December 1980, pp. 267-272.

9. Walker, J.C., and Williams, A.R., "The Improvement of Noise and Traction Due to Road/Tyre Interation", Proceedings of the International Tire Noise Conference, Stockholm, Sweden, August 1979.

10. Walker, J.C., "Tyre-Road Interaction Studies to Improve Noise and Wet Grip", paper presented at ASTM Symposium on Frictional Interaction of Tire and Pavement, November 1981.

11. Anderson, D.G., and Landers, S.P., "On-Board Passenger Tire Sound Generation Study, Road Versus Lab Wheel", SAE Paper 762016, November 1976.

12. Lippman, S.A., and Reid, K.A., "A Laboratory Procedure for Measuring the Sound Level of Truck Tires", SAE Paper 762015, November 1976.

13. Donavan, P.R., and Oswald, L.J., "The Effects of Surface Curvature and Texture on Passenger Car Tire Noise Generation on Roadwheels and Roadways", paper presented at ASTM Symposium on Frictional Interaction of Tire and Pavement, November 1981.

14. Pope, J., and Reynolds, W.C., "Tire Noise Generation: The Roles of Tire and Road", SAE Paper 762023, November 1976.

APPENDIX A

Asphalt Paving Mixtures

These paving mixtures consist of a uniform mixture of coarse aggregate, firm aggregate, asphaltic material, and mineral filler. The grading of each constituent of the mineral aggregate conforms to the following specifications:

OHIO 402	Percent By Weight
Passing 1-inch sieve	100
Passing 3/4-inch sieve	90 to 100
Passing 1/2-inch sieve, retained on No. 4 sieve	65 to 90
Passing No. 4 sieve, retained on No. 16 sieve	35 to 65
Passing No. 16 sieve, retained on No. 50 sieve	15 to 44
Passing No. 50 sieve, retained on No. 200 sieve	3 to 22
Passing No. 200 sieve	0 to 8

The asphaltic material shall form from 4.0 to 9.5 percent of the mixture by weight.

OHIO 404	Percent By Weight
Passing 1/2-inch sieve	100
Passing 3/8-inch sieve, retained by No. 4 sieve	90 to 100
Passing No. 4 sieve, retained on No. 16 sieve	45 to 75
Passing No. 16 sieve, retained on No. 50 sieve	15 to 45
Passing No. 50 sieve, retained on No. 200 sieve	3 to 22
Passing No. 200 sieve	0 to 8

The asphaltic material shall form from 4.5 to 9.5 percent of the mixture by weight.